NSWCDD/TR-93/643

SEAFLOOR POSITIONING ACROSS JUAN DE FUCA RIDGE

BY PATRICK FELL C. HARRIS SEAY
STRATEGIC AND SPACE SYSTEMS DEPARTMENT

APRIL 1994

NAVAL SURFACE WARFARE CENTER
DAHLGREN DIVISION
Dahlgren, Virginia 22448-5100

NSWCDD/TR-93/643

SEAFLOOR POSITIONING ACROSS JUAN DE FUCA RIDGE

BY PATRICK FELL C. HARRIS SEAY

STRATEGIC AND SPACE SYSTEMS DEPARTMENT

APRIL 1994

NAVAL SURFACE WARFARE CENTER

DAHLGREN DIVISION

Dahlgren, Virginia 22448-5100

FOREWORD

This report presents results from an analysis of Global Positioning System (GPS) satellite and marine acoustic observations to extend WGS 84 geodetic control onto the seafloor. The data were collected as part of an experiment in marine geodynamics conducted by the United States Geological Survey (USGS) with support from the University of Hawaii; the Naval Postgraduate School; the Defense Mapping Agency (DMA); the Naval Surface Warfare Center, Dahlgren Division (NSWCDD); and the U.S. Navy Submarine Group One. At NSWCDD, data analysis was performed in the Space and Surface Systems Division of the Strategic and Space Systems Department under sponsorship of the Defense Mapping Agency.

The authors would like to acknowledge Dr. Janet Morton of the USGS in Reston, Virginia, for her dedication in organizing the experiment; Dr. Muneendra Kumar of the DMA who recognized the geodetic opportunity represented by the experiment; Ms. Carol Reiss of the USGS in Menlo Park, California, for providing GPS and acoustic data sets and for explaining many details associated with the USGS data acquisition and processing; Professor Steven Tucker of the Naval Postgraduate School for providing the sound velocity profile used for refraction correction; and Mr. Paul Jackins of NSWCDD who provided software for acoustic ray tracing.

This report has been reviewed by J. L. Sloop, Head, Space and Surface Systems Division.

Approved by:

R. L. SCHMIDT, Head
Strategic and Space Systems Department

ABSTRACT

The results of an analysis of a complex data set acquired during the United States Geological Survey's Marine Crustal Deformation Study are presented. The experiment, which commenced in the spring of 1992 in a region of the Pacific known as the Juan de Fuca ridge, represents a first attempt to locally monitor plate dynamics in the marine environment using a network of tripod-mounted, dual-frequency acoustic transponders. The aim is to collect over a period of years time-series measurements of extension rates along the southern Juan de Fuca ridge. In addition, by collecting a combination of Global Positioning System satellite tracking data, low-frequency acoustics data, and water column pressure, conductivity, and temperature at depth, it was possible to extend geodetic control from land onto the seafloor. The methods to accomplish this latter goal of the experiment are described, as well as the final results. Baseline comparisons between several of the solutions obtained during this analysis are presented along with recommendations for additional data collection and analysis.

CONTENTS

ILLUSTRATIONS

ILLUSTRATIONS (CONTINUED)

TABLES

INTRODUCTION

The long-term goal of extending geodetic control into the oceans is moving closer to becoming a practical reality due to improvements in acoustical instrumentation and through the use of the Global Positioning System (GPS). Recent experimentation in 1991 by the Jet Propulsion Laboratory and the Scripps Institution of Oceanography, University of California at San Diego, followed in 1992 by an experiment organized by the United States Geological Survey (USGS), demonstrates that, although not by any means routine, these combined measurement technologies enable geodetic positioning under the seas to be obtained in a global reference frame.

During the month of May 1992, an acoustic transponder network was deployed across the Juan de Fuca ridge, 300 nmi off the Oregon coast. This experiment sponsored by the USGS and the Defense Mapping Agency (DMA) has a principal goal of monitoring the crustal spreading rate in the marine environment through long-term observation at a fixed seafloor network. A second objective of the experiment was to determine geodetic positions for the deep ocean acoustic transponder network in a global reference frame, thus extending WGS 84[1] geodetic control onto the seafloor. The experiment represents a partnership that includes contributions from the USGS, the University of Hawaii; the Naval Postgraduate School (NPS); the DMA; the Naval Surface Warfare Center, Dahlgren Division (NSWCDD); and the U.S. Navy Submarine Group One.

GEODETIC POSITIONING IN THE MARINE ENVIRONMENT– EXPERIMENT PLANNING

The main focus of the USGS experiment is to acoustically measure, over time, crustal dynamics under the sea. However, NSWCDD and DMA participated with the USGS in the design of this experiment because of an interest in estimating geodetic coordinates for seafloor instrumentation using a combination of low-frequency acoustics and GPS satellite measurements.

Prior to going to sea, an analysis was carried out to investigate the potential benefits of combining GPS satellite-based positioning and acoustics data for determining the geodetic coordinates of points on the ocean floor. This simulation study provided indications of the accuracy that might be expected for seafloor positioning, as well as a design for shipboard data acquisition. Principally, this analysis was performed using the Ohio State University Geometric and Orbital Program[2] software developed at the Ohio State University's Department of Geodetic Science and Surveying, modified by NSWCDD for this marine application.

This ship-track covariance analysis was undertaken to determine how to maximize the geometric strength (figure of merit) of the low-frequency acoustic data acquisition. Four transponders were considered in this simulation in the approximate locations of the planned USGS deployment located at the corners of a square 1 km on a side at a 2200-m depth. Three ship-track

patterns were analyzed in determining an acoustics data acquisition strategy. Each pattern consisted of a square (see Figure 1) augmented with north-south and east-west crossing tracks lying within its boundary, centered within the square. The side lengths for the concentric squares were 1, 3, and 5 km. The squares were centered over the transponder array. In each case, the simulated acoustic range data acquired along the track pattern (square plus crossing tracks) provided 135 equally spaced events. An event is defined as a set of four acoustic range measurements between the ship and the transponder network obtained while GPS data are collected to at least four satellites, completing (conceptually) a double pyramid (see Figure 2). Thus data density was spacially greatest for the 1-km square pattern and least for the 5-km square. The designations for the test patterns were pattern 1 for the 3-km square, pattern 2 for the 5-km square, and pattern 3 for the 1-km inner square. A data simulator was developed that generated acoustic ranges to the transponders from a ship that traversed each track pattern.

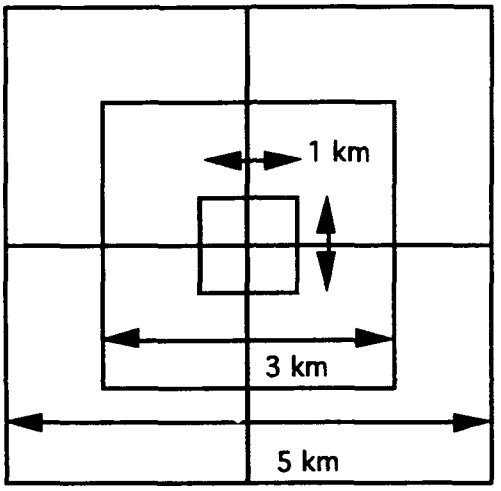

FIGURE 1. SHIP TRACK PATTERNS FOR LOW-FREQUENCY DATA ACQUISITION

These simulated acoustic observations were then processed using a least-squares estimation technique to determine the affect of ship-track geometry on position uncertainty for the array. Results were obtained first for pattern 1 using different constraints on the accuracy of the associated ship positions that would be determined at sea using GPS satellite measurements. The accuracy to which a ship can be positioned, both absolute and relative, varies greatly depending on GPS data types, collection sites, and processing modes. Accuracies of 10 m, 1 m, and 10 cm were considered in this study. Acoustic ranges were assumed to have a 1-m standard error for those slant ranges presented by the ship-to-array geometry. Figure 3 provides the latitude, longitude, and ellipsoidal height uncertainty (1 sigma) for transponder T1 as a function of ship position uncertainty. Results for transponders T2, T3, and T4 were almost identical. These results indicated that ship positioning accuracy of 1 m relative to terrestrial geodetic control would be more than sufficient for the experiment. Improving position accuracy using more involved GPS data acquisition and processing would improve transponder positioning only marginally, this limitation being due to the accuracy of the low-frequency acoustic ranges.

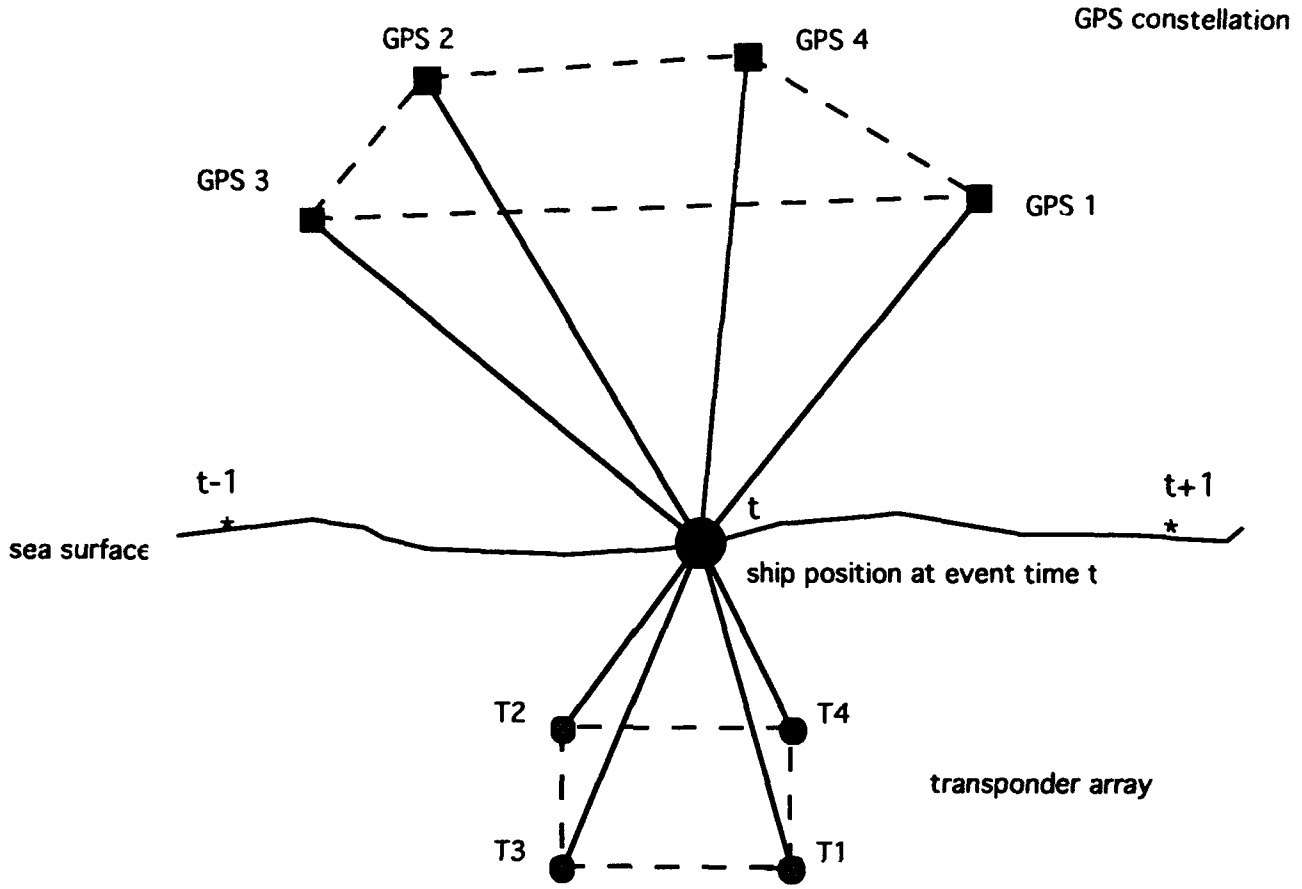

FIGURE 2. DOUBLE PYRAMID GPS/ACOUSTIC EVENT AT TIME t

Subsequent simulations, each with 135 events, were performed for track patterns 2 and 3 however using only 1-m GPS ship position uncertainty. Figure 4 provides these additional results. Pattern 2 (case 2) provided improved geometric strength for array latitude and longitude over track pattern 1, but height uncertainty remained about the same. Acoustic data simulated along pattern 3 (case 3) provided a weaker solution than either patterns 1 or 2 with height uncertainty affected least. Finally, Figure 4 provides the results when data from all three track patterns were combined (case 4). These 405 events in the combined solution (1620 acoustic ranges) were distributed with a higher density close to the array. Observation density then decreased as the distance from the array increased. The combined result gave standard errors for the array of approximately 16, 28, and 10 cm, respectively, for the latitude, longitude, and ellipsoidal height of each transponder instrument. The difference in the latitude and longitude uncertainties was a result of placing the GPS position uncertainty of 1 m on the Cartesian coordinates of the ship's positions rather than on geodetic coordinates. The combined result is better than transponder uncertainty resulting from the use of 10-cm GPS positioning with data from any one single track pattern having 35 events (compare Figures 3 and 4). Thus an increase in acoustic data acquisition using multiple tracks seemed preferable to obtaining the most accurate GPS positioning possible and would reduce requirements for more complex GPS data acquisition and processing.

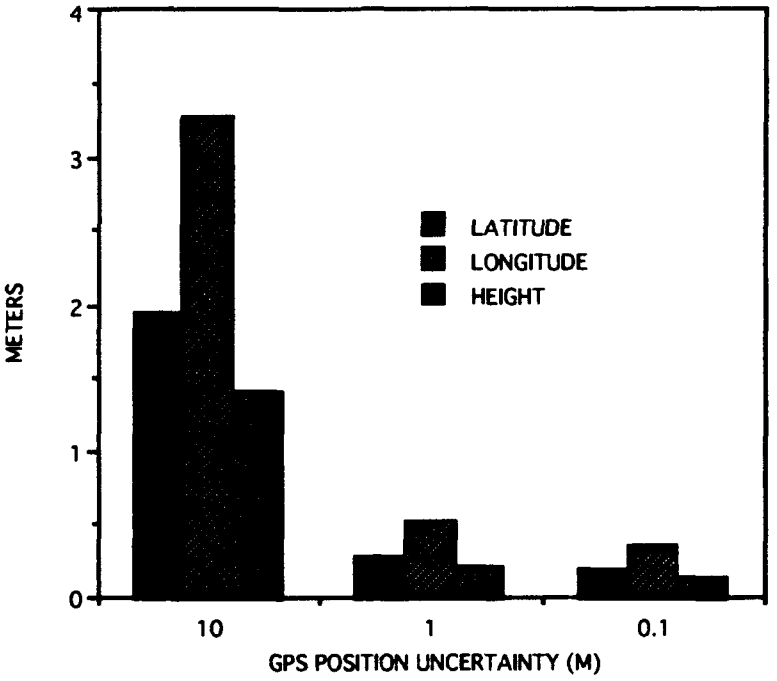

FIGURE 3. TRANSPONDER ARRAY UNCERTAINTY VS. GPS POSITIONING UNCERTAINTY FOR TRACK PATTERN 1

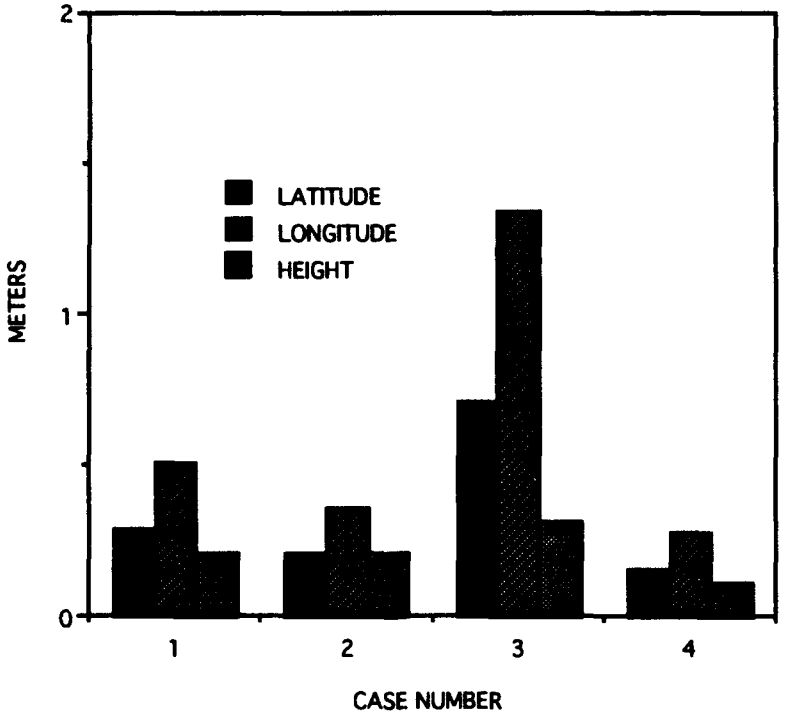

FIGURE 4. TRANSPONDER UNCERTAINTY ASSOCIATED WITH 1-M GPS SHIP POSITIONING; CASE (1): PATTERN 1, CASE (2): PATTERN 2, CASE (3): PATTERN 3, CASE (4): COMBINED SOLUTION

Track patterns 1, 2, and 3 together represent a total of 46 km of ship track. With some redundancy and extra tracking to connect the three patterns, the entire track set could be collected in 6 hr if the ship were to transit the approximately 53-km distance at an average speed of 8.8 km/hr. However, restrictions on the acoustic data acquisition speed of the ship would need to be taken into account for final planning.

GPS availability during the data collection period would be able to support continuous four or four-plus satellite coverage for relative positioning of the ship. Ship position accuracy as a function of time for the available GPS satellite coverage however was not considered in this analysis. It was believed that sufficient GPS coverage would be available during the data acquisition phase of the experiment to obtain sufficient accuracy relative to a fixed land site at Newport, Oregon. There were no requirements to collect all acoustic and GPS data in a single session. The ship collection could be performed in segments over several days.

These study results indicate the potential power of combining GPS observables and acoustic ranges to obtain undersea geodetic positions for points of interest. It is believed that this approach represents the most likely future technology to extend geodetic control into the ocean environment. However, this study did not consider the effect of systematic errors such as in GPS ship positioning or in acoustic refraction correction. It can therefore only provide (optimistic) results reflecting the geometric contributions to such a solution as a guide for data acquisition.

USGS MARINE GEODYNAMICS EXPERIMENT

EXPERIMENT BACKGROUND

The USGS deployed four dual-frequency Oceano SI-431-3 acoustic transponders in tripods southwest of an area containing low-frequency Benthos transponders previously deployed by the National Oceanic and Atmospheric Administration (NOAA). The site selected for the deployment was 300 nmi west of Astoria, Oregon at a point along the Juan de Fuca ridge where crustal spreading rates were estimated to be 6 cm per year. Of the four transponders deployed, three functioned properly, providing an extensive acoustics data set over a two-day calibration period. Acoustics data were also collected from several of the NOAA instruments. Figure 5 provides the locations of the four USGS instruments and the location of one NOAA transponder whose data were analyzed in this study. Notice in Figure 5, and in the following, that the transponder designations T5, T6, T7, and T4 are consistent with USGS data files and not with notations used in the previous section on experimental planning.

The experiment, as it pertained to precise seafloor positioning, consisted of collecting several types of data over a common time interval, then using this data to transfer geodetic control from land onto the seafloor. Figure 6 provides the general layout of the experiment data collection. Details on the specific data sets follow.

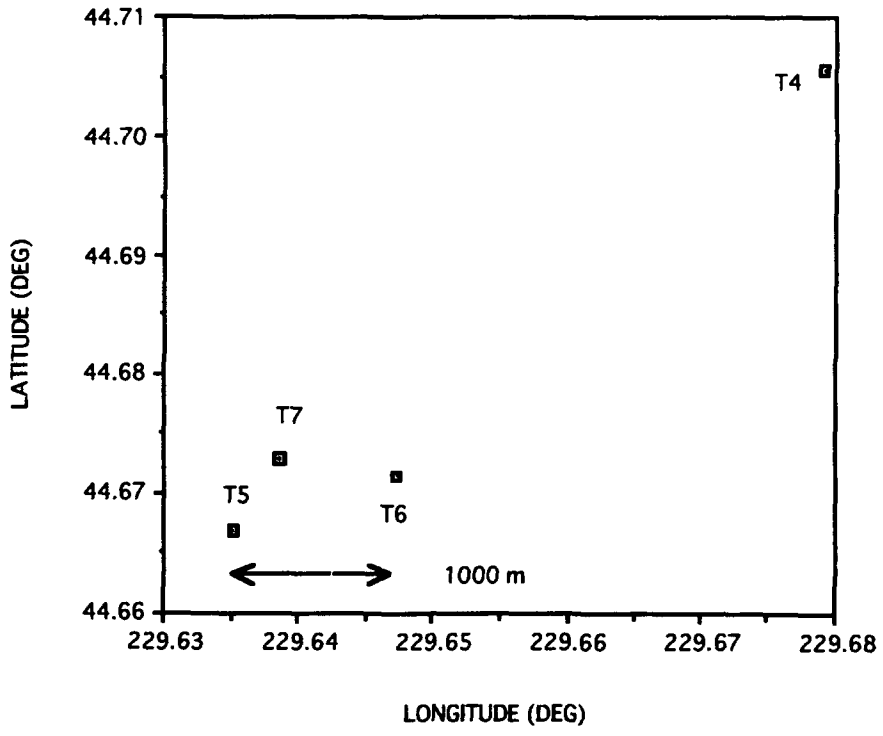

FIGURE 5. LOCATION OF USGS TRANSPONDERS (T5, T6, T7) AND NOAA TRANSPONDER T4

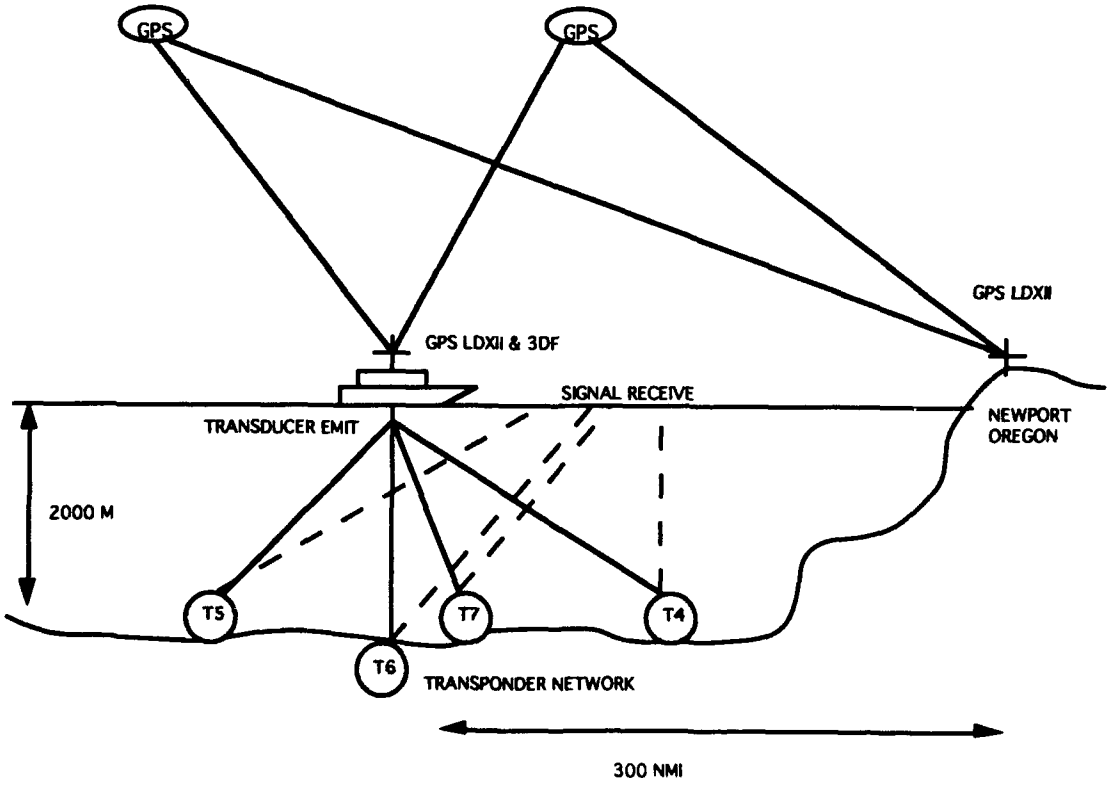

FIGURE 6. DATA ACQUISITION DURING USGS JUAN DE FUCA RIDGE EXPERIMENT

RELATIONSHIP TO EXPERIMENT PLANNING

Although a large data set was acquired during the calibration period, after collation and editing, the actual geometry of the remaining ship tracks above the USGS array covered an area most analogous to track pattern 3 considered earlier. Therefore, the data set used in the latter parts of this study lacked the geometrical strength associated with the broader collection patterns previously studied. This issue will be considered when the results from the data analysis are interpreted.

INSTRUMENTATION AND DATA COLLECTION

Data collected aboard the Navy Deep Submergence Vehicle *Turtle* and Support Ship *Laney Chouest* during the site visit included dual- and single-frequency pseudorange and carrier phase observations from shipboard Ashtech LDXII and 3DF GPS receivers providing ship location and three-dimensional ship attitude, low frequency (8–16 kHz band) acoustics between the vessel and the transponder network providing round-trip travel times between the survey ship and the USGS and NOAA transponders, and direct measurements of electrical conductivity, temperature, and pressure within the water column to determine a sound velocity profile. Because of a failure of the Oceano RM-201 range meter, high frequency (50-108 kHz band) intersite acoustic range data acquisition was commanded between the USGS transponders; however, data retrieval was not possible. This latter data will eventually be retrieved to provide direct measurement of crustal dynamics. It will also serve to validate the geodetic positioning results from this analysis. In addition, a fixed GPS land site, station *VENTS*, at the Hatfield Marine Science Center in Newport, Oregon, was occupied with a dual-frequency Ashtech LDXII GPS receiver to support differential positioning of the ship relative to known geodetic control. Although data were collected over several days, the data analysis was confined to calibration lines that spanned a period that began at hour 18 on day 142 and finished at the end of hour 3 on day 143. Because the different data types were not consistently collected over the same periods, the entire acoustics data set could not be fully exploited. Figure 7 illustrates the time intervals during days 142 and 143 when various data sets were collected.

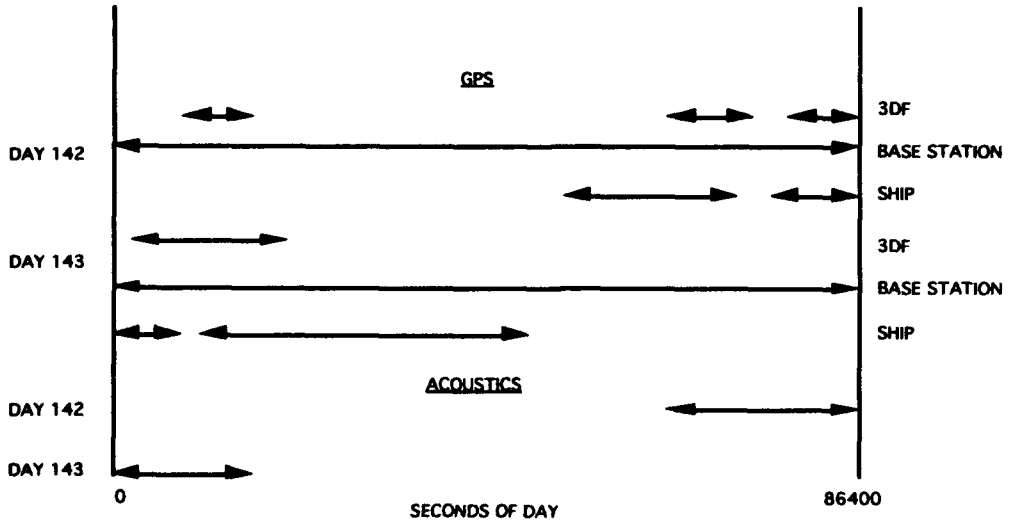

FIGURE 7. CALIBRATION TRACKS FOR JUAN DE FUCA RIDGE EXPERIMENT–DATA COLLECTION INTERVALS ON DAYS 142 AND 143

PRELIMINARY DATA PROCESSING AND DATA EDITING

After receipt of the data sets collected aboard the *Laney Chouest* and the GPS tracking data acquired at Newport, Oregon, several data processing steps were undertaken. These included editing acoustics data to remove multiple returns, processing GPS receiver range measurements to position the ship relative to known geodetic control on land, examining acoustics data residuals to eliminate questionable data, evaluating interpolating schemes to determine ship location at acoustic signal receive times, connecting GPS antenna locations to the transducer through the use of GPS-derived ship attitude data, and editing data sets to produce complete data coverage over selected time intervals. Several of these procedures were executed at the beginning of the data processing, others were added as the data analysis proceeded, refining methods and including more complete modeling. The following paragraphs summarize these procedures.

INITIAL EDITING TO REMOVE MULTIPLE RETURNS

Each transponder within the USGS and NOAA arrays operates with a unique response frequency. The frequencies of the transponders whose data were processed in this study are given in Table 1, along with their approximate positions. During a first evaluation of the acoustics data collected aboard ship, it was readily evident that the data files consistently contained multiple (up to four) returns from each transponder. This was clearly a result of multiple reflections of the transmitted acoustic signal off the seafloor and ocean surface, which then triggered additional chirps from the transponder instrumentation.

Using approximate locations for the transponder and ship positions, an initial editing of all acoustic data was completed to identify and eliminate all but principal returns from each transponder associated with a 20-sec transducer pulse rate. These edited files, configured on an hourly basis, represented the source data for all subsequent processing steps.

TABLE 1. TRANSPONDER INFORMATION

Instrument Number	Latitude* (deg)	Longitude* (deg)	Depth (m)	Frequency (Hz)
NOAA 04	44.706	229.679	-1987	13000
USGS 05	44.667	229.635	-2205	11500
USGS 06	44.671	229.647	-2205	12000
USGS 07	44.673	229.639	-2205	12500

*Approximate position in WGS 84

GPS SHIP POSITIONING

GPS ship positioning was accomplished using the Ashtech software program *PPDIFF*, which was designed to differentially post-process navigation solutions collected in the field. Since an initially known baseline was not established, an alternate processing program GPPS for the kinematic mode was not used. GPPS would have been more desirable from an accuracy standpoint because it could have used precise GPS ephemerides. PPDIFF required the raw measurements that were downloaded from the GPS receivers located at the base station and onboard the ship, as well as the broadcast GPS ephemerides.

The accuracy of the results from PPDIFF were expected to range from 5 to 15 m under optimal conditions over the distances present in this experiment. Errors due to positioning were expected to be systematic (correlated) because of errors in the GPS ephemerides.

RESIDUAL EDITING

Acoustic data sets known as calibration lines were placed in single hour files beginning on day 142, hour 18 and ending after day 143, hour 3. The data files initially contained a ship position for each signal transducer pulse time (20-sec epochs) in a local reference frame. Ship positions in this frame were estimated using acoustics data collected from four of the NOAA transponders whose coordinates in this local frame were previously defined. The local frame was defined by the directions east, north, and down, with its origin on the ocean surface.

During data processing, it was necessary to edit out spurious data points and to determine appropriate weighting for the data. This was done by performing initial adjustments of ship and transponder coordinates and computing means and standard deviations for the residuals of fit. Once computed, these statistics served as a basis for refining the weighting of the data and as a means to edit (remove) data values whose residuals exceeded a linear combination of the mean and a selected multiplier of the standard deviation. Since a systematic, unmodeled signal was generally present in the residuals of each hourly data set, the multiplier used to edit data in each adjustment was heueristically determined. Examples of these editing criteria are presented in the following paragraphs.

SHIP POSITION INTERPOLATION

Acoustic data were collected using a 20-sec transducer pulse rate. The principal returns from the transponders occurred within 3 to 6 sec after the transducer pulse event depending on ship location. After completion of GPS data processing to determine ship position, acoustic data files were modified to include interpolated GPS ship positions at pulse emit times. These GPS positions in WGS 84 were determined using an eight-point Lagrangian interpolation routine that operated on the GPS ship position files. The interpolated values were then substituted into the acoustic data files for positional information in the local reference frame as provided by the USGS. These GPS ship positions were thus developed at the same resolution as the original acoustics data, not at the 1-sec resolution of the actual GPS data.

Although this reduced the number and size of the working data files, several disadvantages resulted from this procedure or were present due to other circumstances. First, the schedule of operation of the dual-frequency GPS receiver on the ship did not always correspond to acoustics data collection intervals (see Figure 7). Thus a significant percentage of the acoustics data were not processed beyond this step due to a lack of GPS positioning support. Second, because of a downloading error aboard ship, only single-frequency GPS positioning from the Ashtech 3DF receiver was available to support calibration line data reduction for day 142. Third, since an eight-point interpolator was used, some GPS position solutions on each end of a continuous span were not available.

In addition, ship maneuvers during any 20-sec time span and breaks in the available GPS or acoustics data sets impacted the procedure used to determine ship position at acoustic signal receive times. This procedure estimated the ship velocity vector from interpolated GPS ship positions at consecutive 20-sec pulse epochs and then extrapolated ship position forward to pulse receive times using this estimated vector. Later, this approach was replaced by the direct use of the Ashtech 3DF receiver data.

The Ashtech 3DF receiver produces, among other quantities, estimates of ship speed and course-over-ground. The latter quantity differs from estimated ship heading insofar as it relates to the orientation of the ship velocity vector not to the orientation of the ship centerline. These quantities can differ by several degrees depending on ship maneuvers, currents, and other conditions. In the latter phases of data processing, the 3DF estimates of speed and course-over-ground were used to extrapolate ship position from pulse emit to pulse receive times for each measurement event.

CONNECTING THE GPS ANTENNA AND THE ACOUSTIC TRANSDUCER

To provide additional completeness in the observation equation, it was necessary to account for the fact that the GPS antenna to which the ship position solutions refer was mounted several decks above the waterline; whereas, the acoustic transducer was mounted below the hull. Since the ship was constantly undergoing changes in roll, pitch, and heading, it was necessary to determine the instantaneous orientation of the displacement vector connecting these points in the WGS 84 reference frame. The GPS ship positions were then transferred to the transducer via vector addition.

For this deployment, the ship dual-frequency GPS antenna was antenna 1 of the four-antenna array connected to the Ashtech 3DF attitude receiver. Antenna 1 was located 16 ft to the port of the ship's centerline, and 5 ft aft of the transducer point. The transducer was located 2 ft starboard of the centerline of the ship. When deployed, it is extended 4 m below the hull. Figures 8 and 9 provide the geometry relating the transducer location (retracted) and GPS antennas 1 and 2. In the ship-fixed reference frame, the vector from antenna 1 to the transducer (retracted position) is given by the components (-18.0, -5.0, 32.5) in units of feet. When the transducer was deployed, the z-component of this vector was modified to reflect its extension away from the hull.

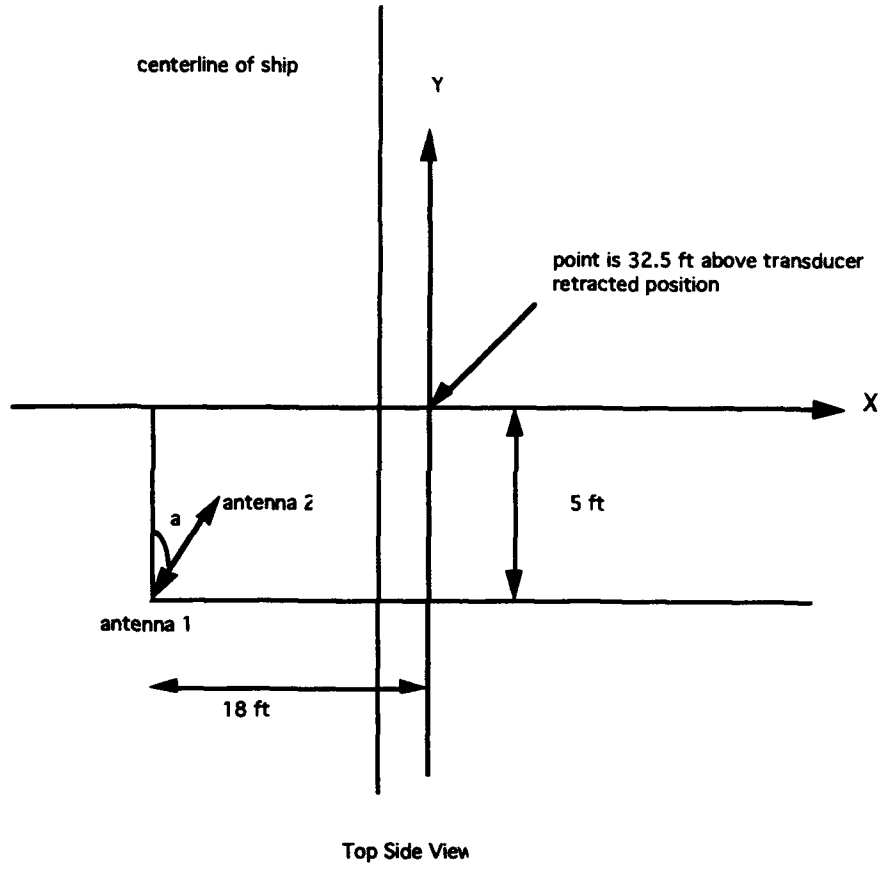

FIGURE 8. LOCATION OF GPS ANTENNAS 1 AND 2 RELATIVE TO TRANSDUCER ON HULL

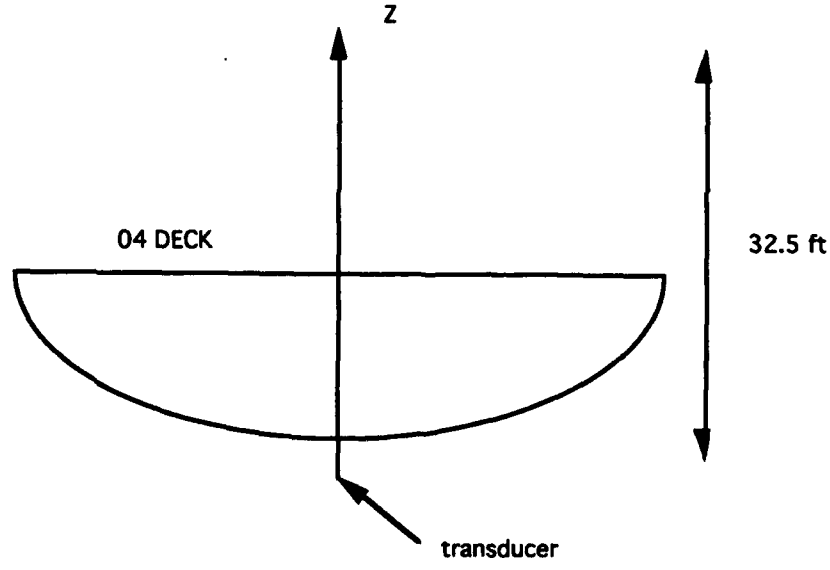

FIGURE 9. TRANSDUCER LOCATION (RETRACTED)

The Ashtech 3DF receiver collects C/A single-frequency GPS range and phase observations using a four-antenna array and produces a three-dimensional attitude history for the plane containing the antenna array. In this particular configuration, the antennas were deployed on different decks of the ship and were not aligned to the ship centerline. Therefore, adjustments needed to be applied to the 3DF attitude results to determine the roll, pitch, and heading of the ship. After considering the relative locations of the antennas on the ship's decks, it was determined that the pitch, roll, and heading offsets of the antenna array relative to the body-fixed axes of the ship were -18.6, -0.5, and -3.1 deg, respectively. The 3DF attitude data were corrected to reflect the attitude dynamics of the ship reference frame.

To determine the position of the transducer in the WGS 84 reference frame, a set of rotation matrices had to be applied to transform the ship-fixed displacement vector between antenna 1 and the transducer into the WGS 84 frame. This rotation was accomplished using the following transformation equation.

$$X_{WGS\ 84} = R_Z(-(180+\lambda))R_Y(90-\varphi)R_Z(90+\phi)R_X(-\varphi_p)R_Y(-\psi)X_{ship} \quad (1)$$

where

$$X_{WGS\ 84} = (x,y,z)_{WGS\ 84} \quad (2)$$

and X_{ship} are the Cartesian coordinates of the antenna-transducer displacement vector in the body-fixed (ship) frame. This transformation equation consists of a rotation into the north-east-up frame followed by a rotation into the geodetic reference frame. The rotation angles ψ, φ_p, ϕ, φ, and λ used in this transformation are the roll, pitch, heading, latitude, and longitude, respectively, of the ship. All angular quantities are derived from the GPS observables. The rotation matrices R_X, R_Y, R_Z are the standard Euler angle rotations.[3]

Once the displacement vector is known in WGS 84, it is added to the WGS 84 Cartesian coordinates of antenna 1, determined using dual-frequency GPS observables, to yield the WGS 84 Cartesian coordinates of the transducer at emit or receive times.

EDITING TO PRODUCE COMMON DATA INTERVALS

Figure 7 shows that the data collection interval during this experiment was not consistent across data types. As various phases of acoustics data processing were performed, as discussed in detail, the volume of the acoustics data considered varied depending on the degree to which it could be supported by the availablity of other data types. All data sets were edited at each step in the processing to produce the largest common data interval for that processing phase.

INITIAL ADJUSTMENT RESULTS

A first adjustment using only acoustics data was performed incorporating all data files with the exception of hour 0 on day 143. This one data set was not initially processed because of some difficulty with reading the file on the CDC 995 system. A total of over 7000 acoustic observations were processed. These data were acquired from the three USGS transponders (T5, T6, T7) and one NOAA transponder T4 (see Figure 5). Initial coordinates for transponder and transducer positions were provided by the USGS in a local reference frame in which the NOAA transponder coordinates were known. The adjustment assigned an initial uncertainty of 5 m to each acoustic observation and a position uncertainty of 20 m to each ship position coordinate. The ship tracks during this calibration line collection period are shown in Figure 10.

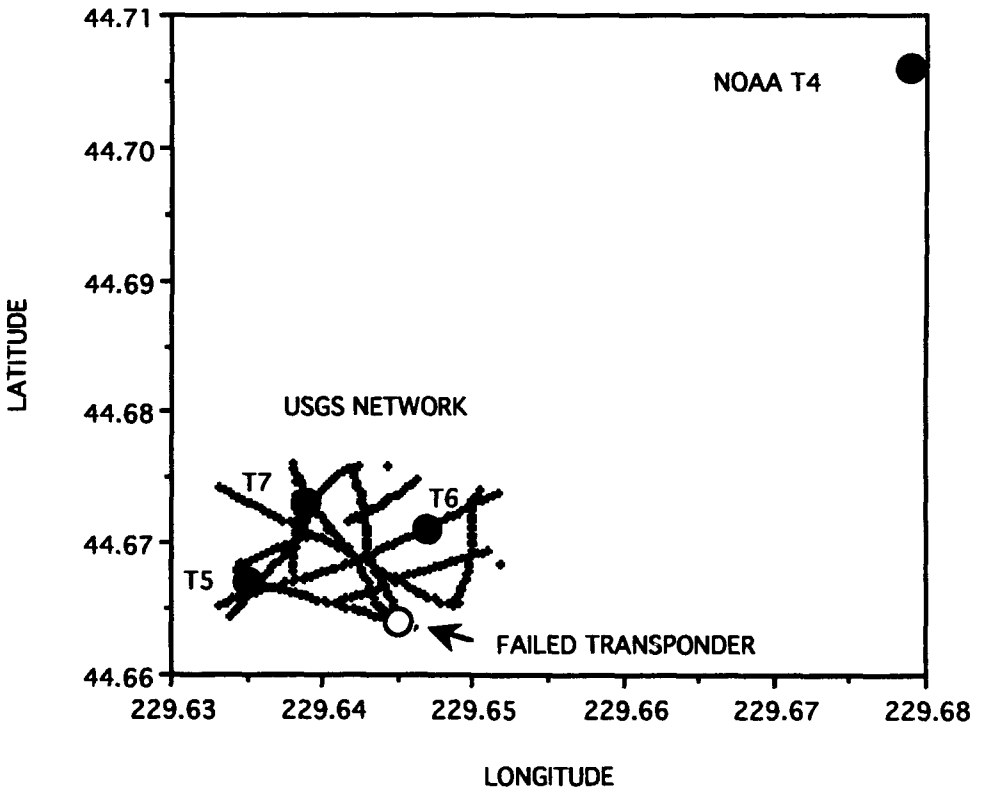

FIGURE 10. CALIBRATION LINE SHIP TRACKS OVER USGS TRANSPONDER ARRAY ON DAY 142, HOUR 18 TO DAY 143, HOUR 3

The purpose of this initial adjustment was to examine the internal consistency of the data set, to establish a basis for data editing using residuals of fit, and to determine appropriate data weighting for subsequent adjustments. The starting transponder coordinates and the resulting adjustments to these coordinates are given in Table 2.

TABLE 2. STARTING TRANSPONDER COORDINATES* AND RESULTS FROM INITIAL ADJUSTMENT
(units in meters)

Unit	X	Y	Z	ΔX	ΔY	ΔZ
T5	11974	14137	2205	-2.0	-4.6	7.3
T6	12902	14627	2205	-1.8	5.7	11.3
T7	12240	14800	2205	8.3	-2.4	10.3
T4	15443	18396	1987	8.8	-4.7	31.8

*Local reference frame

Several assumptions were made at this stage in the processing and important corrections to the data had not been applied. For instance, acoustic refraction corrections could not yet be computed because the necessary sound velocity profile was not available from NPS, therefore a constant sound velocity of 1482.62 m/sec was used for data processing initially. Also, a transponder internal electronic delay of 0.015 sec was adopted for each instrument as suggested by USGS. These factors are the most likely causes for the z-coordinate (downward) adjustment in Table 2 for all transponders units.

Figure 11 illustrates the adjustments occurring to the initial coordinates for the transponders as the normal equations were sequentially merged and solved. This scheme was followed beginning with the normal equations for calibration track 18 (hour 18, day 142) through track 03 (hour 3, day 143). Figure 11 shows the results at several stages of this process; the last step 18-03 being the solution based on all acoustics data with the exception noted above. For the coordinates of transponders T5, T6, and T7 these sequential adjustments were more consistent (clustered) than for the more distant NOAA unit T4.

Figure 12, corresponding to Figure 11, provides the coordinate covariance evolution as track data were merged. Although not necessarily a valid representation of the statistical uncertainty for the solution, these numerical values do provide some general insight into the data set's ability to provide accurate positioning: first, the data set supports a stronger solution for depth than it does for the horizontal coordinates of the USGS array; and second, the ability to position the more distant NOAA transponder T4 is much weaker due to the actual geometry of the data acquisition.

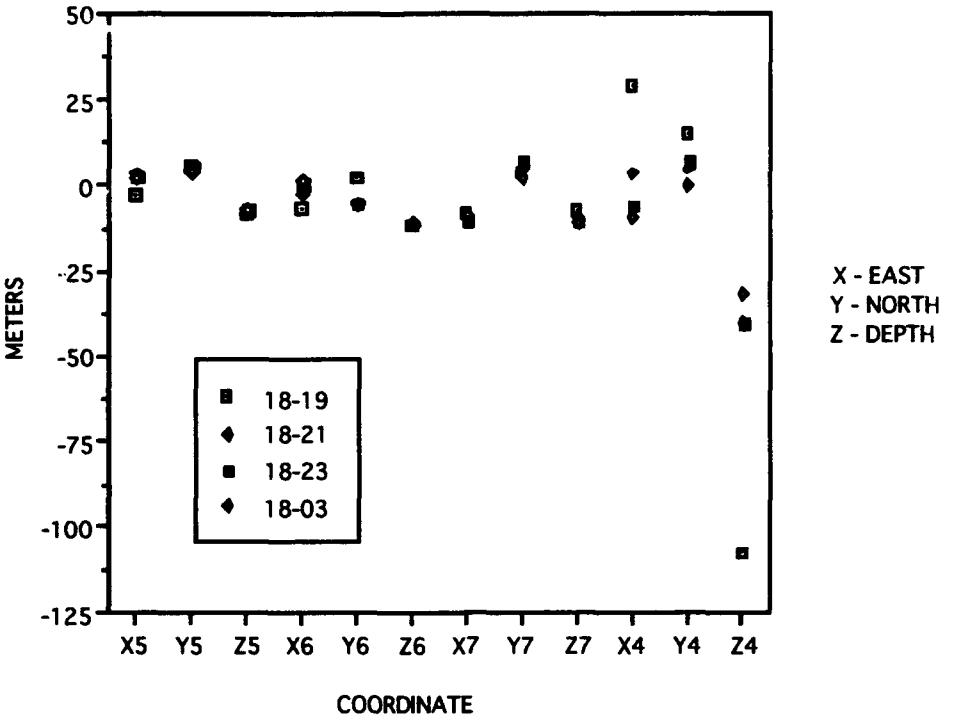

FIGURE 11. INITIAL ACOUSTIC DATA SOLUTION–COORDINATE ADJUSTMENTS AS CALIBRATION LINE DATA ARE MERGED

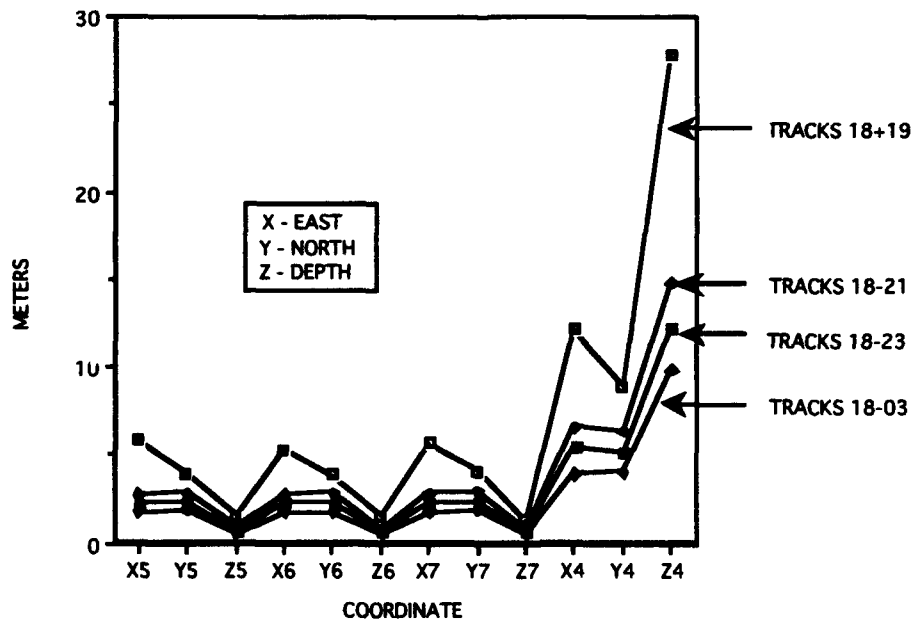

FIGURE 12. COORDINATE COVARIANCE AS TRACK DATA ARE MERGED

This adjustment also provided a significant view into the nature of the acoustics data. Figures 13 and 14, for example, are plots of the post-adjustment data residuals for two of the calibration tracks. Although there are systematic trends in the residuals evident for each transponder, it can readily be seen that spurious data points and large systematic errors are present. Each of the acoustic files was then edited to eliminate suspect data. Figures 15 and 16 are two examples of the residuals of fit after data editing, prior to a second adjustment using edited acoustic data sets.

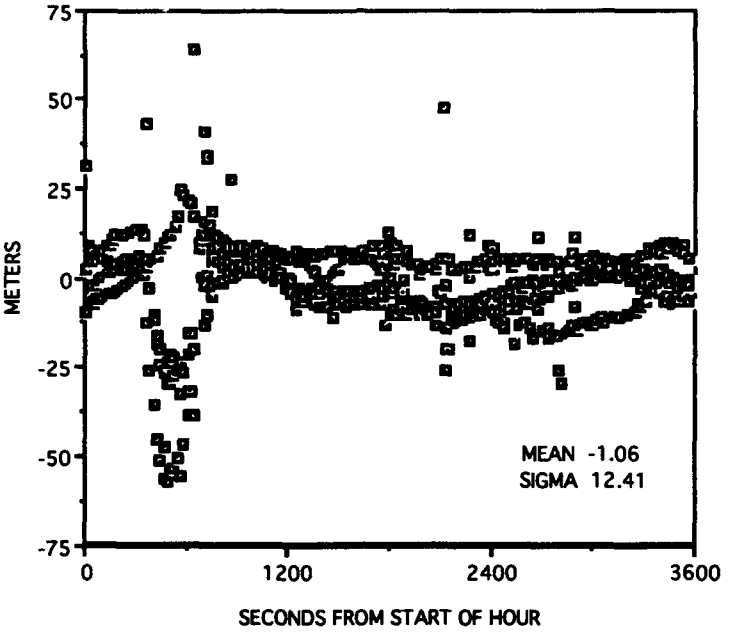

FIGURE 13. POST-ADJUSTMENT RESIDUALS (HOUR 19)

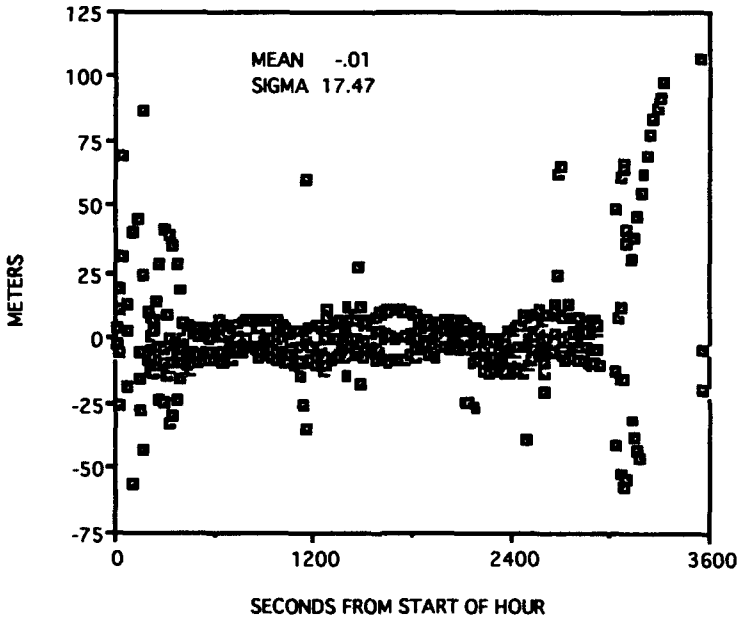

FIGURE 14. POST-ADJUSTMENT RESIDUALS (HOUR 23)

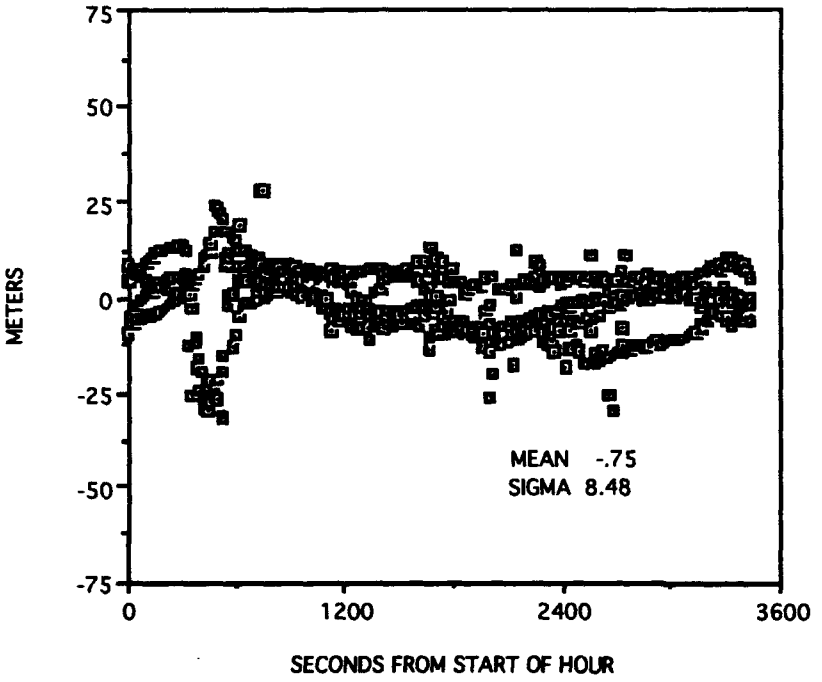

FIGURE 15. EDITED POST-ADJUSTMENT RESIDUALS (HOUR 19)

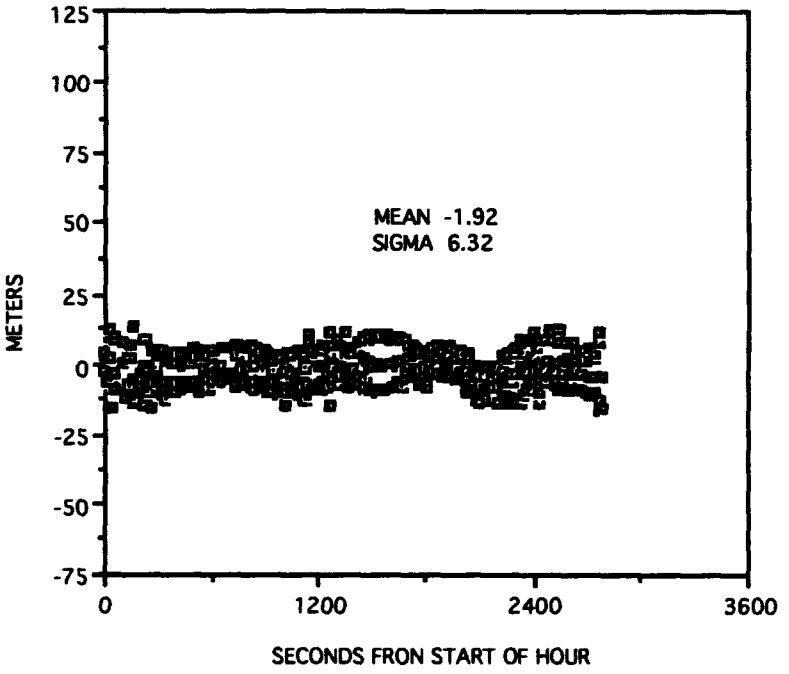

FIGURE 16. EDITED POST-ADJUSTMENT RESIDUALS (HOUR 23)

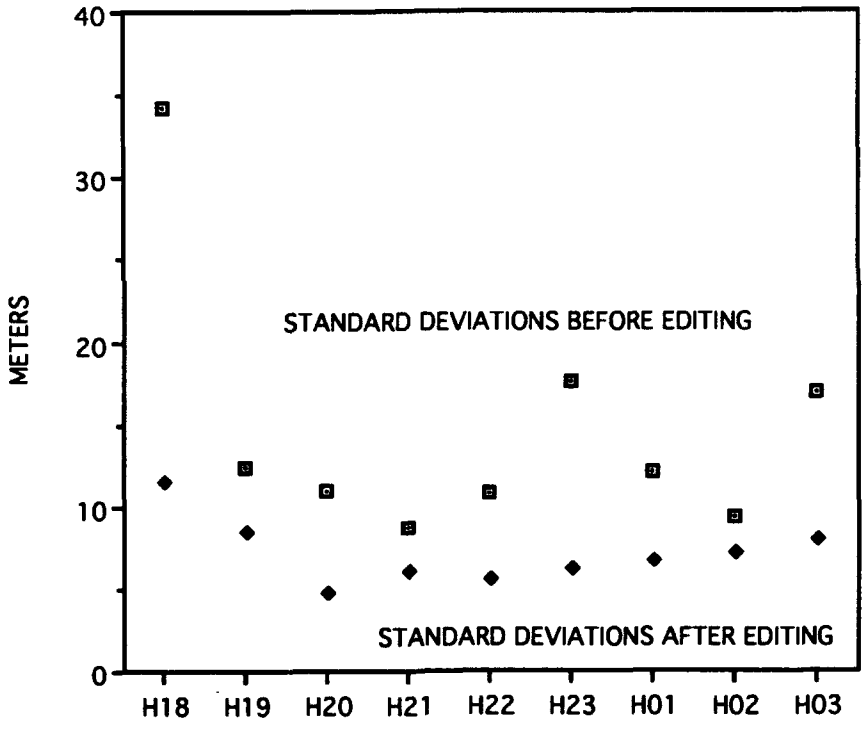

FIGURE 17. STANDARD DEVIATIONS OF HOURLY ACOUSTICS DATA SETS BEFORE AND AFTER EDITING

The mean and standard deviation of each hourly data set were computed prior to and after data editing using values for the coordinates from the initial adjustment. Table 3 provides these results. The data set multiplier given in the Table 3 was the factor by which the standard deviation of the pre-edited data was multiplied to establish a data rejection (editing) criteria. In general, it appears that the low-frequency acoustics data, after being converted to two-way ranges using a fixed sound velocity, have standard errors of from 5 to 12 m prior to correcting for other factors such as anomalous refraction effects.

TABLE 3. HOURLY DATA SET STATISTICAL MEASURES, PRE- AND POST-EDITED
(units in meters)

Hour	Mean	Sigma	Edited Mean	Edited Sigma	Multiplier
18	3.9	34.3	0.1	11.5	3.0
19	-1.1	12.4	-0.8	8.5	2.5
20	2.0	11.0	0.7	4.9	2.5
21.	-1.3	8.7	-1.4	6.1	2.5
22	-1.3	10.7	-0.8	5.6	2.5
23	0.0	17.5	-1.9	6.3	1.0
01	-1.5	12.0	-1.9	6.7	1.5
02	-0.1	9.4	-0.8	7.2	2.5
03	-0.2	16.8	-0.5	8.0	1.5

A second adjustment was then made using these edited files. This adjustment was performed using exactly the same conditions as the first but included only the edited data sets. Table 4 shows the impact of data editing on the parameter adjustments. Significant changes to some of the parameters resulted, implying that data editing would be critical to obtaining a final solution.

TABLE 4. RESULTS FROM INITIAL ADJUSTMENT AND ADJUSTMENT USING EDITED ACOUSTICS DATA
(units in meters)

	Initial Adjustment			Adjustment Using Edited Data		
Unit	ΔX	ΔY	ΔZ	ΔX	ΔY	ΔZ
T5	-2.0	-4.6	7.3	-3.1	4.5	1.4
T6	-1.8	5.7	11.3	-5.1	4.9	3.5
T7	8.3	-2.4	10.3	10.2	-9.2	3.9
T4	8.8	-4.7	31.8	-13.3	-4.4	26.7

ADJUSTMENT INTO THE WGS 84 REFERENCE FRAME

Even though these initial solutions provided good insight into the characteristics of the acoustics data, they are of little value to those interested in geodynamics or geodetic positioning because they are not linked to any global reference frame. Ideally, the positions of these instruments would be known with high accuracy in a well-established global reference frame so that, in the future, any detected spreading rates derived from high-frequency acoustics could be expressible as a vector quantity in the same frame. This would allow a more comprehensive merging of such marine experimental results with terrestrial geodynamical findings. This is where GPS plays a critical role.

As described, the USGS Juan de Fuca ridge experiment was supported by two dual-frequency GPS receivers, one antenna located on an upper deck of the *Laney Chouest* and a second located in Newport, Oregon at a point of known geodetic control in WGS 84. The data collection at the two receivers allowed the ship's track to be determined in the WGS 84 reference frame with an accuracy sufficient for processing the acoustics data set. Since the ship positions derived from GPS are in the WGS 84 reference frame, their use in the acoustics data processing as weighted parameters ensures that the transponder coordinates are determined within the same geodetic system.

At this stage in the data analysis, two additional solutions were made supported by GPS-derived ship positions. The first (I) included all acoustics data acquired on day 142 beginning at hour 18 and ending on day 143 at hour 3 with the exception of hour 0. The second (II) included only the data used in the first solution acquired during day 143, hour 1 to hour 3. Again, as in the acoustics data solutions described earlier, refraction corrections were not applied. In addition, the relationship between the ship's GPS antennas and the transducer's position was purposefully neglected at this stage, since the Ashtech 3DF data for day 142 had not yet been received. Both solutions used the edited acoustics data (edited to remove spurious observations and acoustics data

when GPS solutions were not available (see Figure 7)). Each solution used data weighting consistent with sample statistics developed from examining previous residuals of fit.

These solutions were processed assuming that the GPS ship positions were accurate to 20 m. As it turned out, on the ship at the end of day 142, the GPS data was downloaded to tape. However, instead of downloading dual-frequency data, only single-frequency Ashtech 3DF data were recorded on tape. Both of the GPS ship-based receivers were connected to antenna 1 of the Ashtech 3DF system. This mistake resulted in the loss of dual-frequency data on day 142 so that the first GPS/acoustics data solution had a mix of GPS single-frequency and dual-frequency determined ship positions. After processing the acoustics data on a hourly basis, the normal equations were appropriately merged to produce the two solutions in the WGS 84 reference frame. The second solution based on dual-frequency GPS contained significantly less data.

To compare these GPS-based solutions with the acoustics (edited data) solution in a local reference frame, baseline distances were computed in each frame. The invariant nature of this quantity with respect to reference frame makes it useful for this purpose. Figure 18 provides the baseline lengths from these three solutions. Figure 19 provides the differences in these baseline lengths. Table 5 summarizes these and other solutions performed during this study.

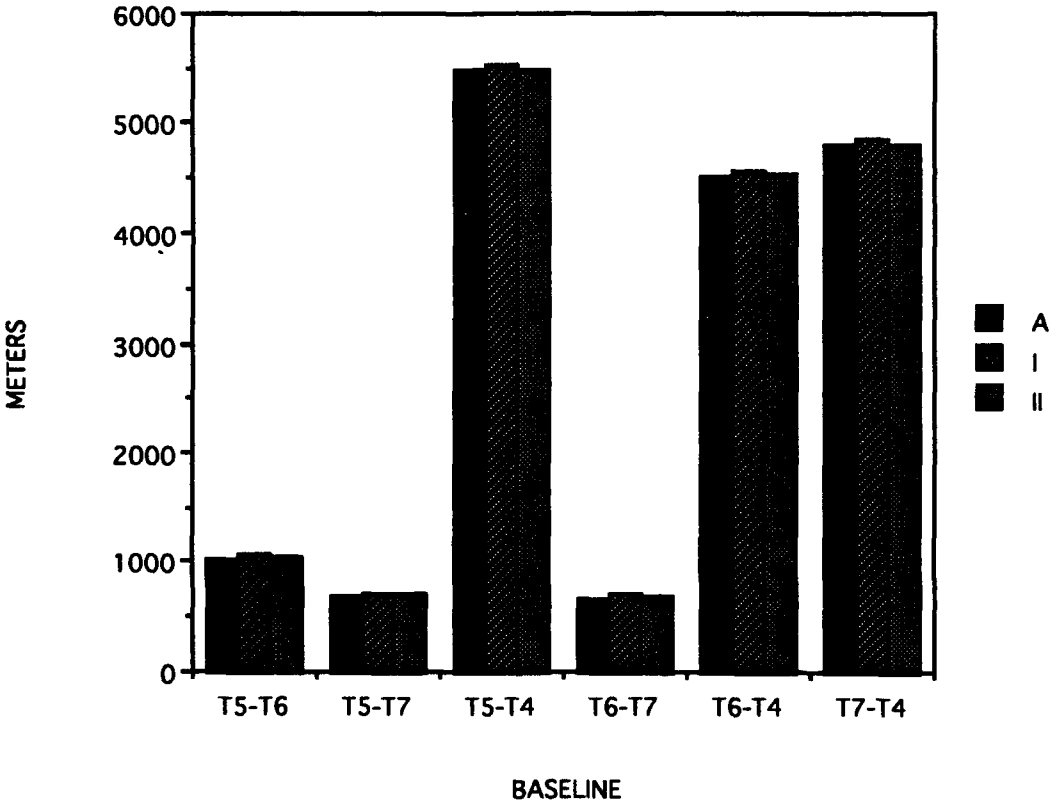

FIGURE 18. BASELINE LENGTHS FROM PRELIMINARY SOLUTIONS

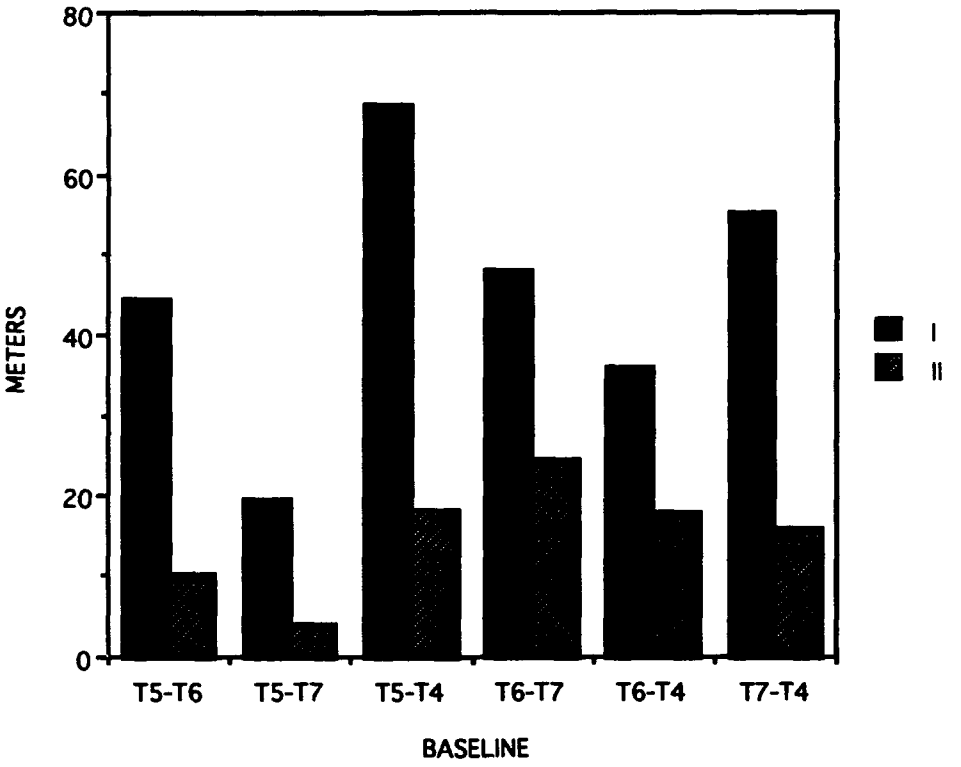

FIGURE 19. BASELINE LENGTH DIFFERENCES FROM PRELIMINARY GPS SOLUTIONS WHEN COMPARED TO ACOUSTICS-ONLY SOLUTION (A)

TABLE 5. SOLUTION SET DEFINITIONS: TRANSPONDERS T5, T6, T7, T4 (DAY 142, HOUR 18 TO DAY 143, HOUR 3)

Designator	Acoustics	GPS Position		GPS Attitude	Refraction Correction
		Transmit Time	Receive Time		
A	18–03 No Hour 00	No	No	No	No
I	18–03 No Hour 00	Day 142 L1 Only Day 143 L1 & L2	Interpolate using GPS 20-sec solutions	No	No
II	01–03	L1 & L2 Solution	Interpolate using GPS 20-sec solutions	No	No
III	01–03	L1 & L2 Solution	Interpolate using GPS 20-sec solutions	Yes	No
IV	01–03	L1 & L2 Solution	Use GPS-derived speed and course	Yes	No
V	00–03	L1 & L2 Solution	Use GPS-derived speed and course	Yes	No
VI A	00–03	L1 & L2 Solution	Use GPS-derived speed and course	Yes	Yes
VI B*	00–03	L1 & L2 Solution	Use GPS-derived speed and course	Yes	Yes

*Solution includes T5, T6, and T7 coordinates only.

The results provided in Figure 19 imply that the use of single-frequency GPS differential positions for the ship at a range of 300 nmi may not prove to be satisfactory. Although the amount of acoustics data present in the first GPS solution is greater than the second solution, the average baseline difference was 45.4 m as compared to 15.2 m resulting from less data but supported by dual-frequency GPS differential positioning. Notice that in each, the scale of the solution is excessive when compared to the acoustics solution in the local reference frame.

SHIP ATTITUDE DATA

In the previous solutions, the relationship between the GPS antenna 1 connected to both the Ashtech 3DF and LDXII receivers and the hull mounted transducer had been ignored. During the next stage of data processing, the 3DF attitude results providing the real-time geometry of the antenna-to-transducer displacement vector were incorporated into the observation equation.

The edited acoustic data files on day 143, hours 1–3, containing dual-frequency GPS ship positions, were augmented with 3DF-derived values of ship heading, pitch, and roll at each transducer emit time. The vector between antenna 1 and the transducer, determined in the ship body-fixed system, was transformed using equation (1) into the WGS 84 reference frame. This displacement vector was then added to the position vector of antenna 1 derived from GPS measurements to determine the WGS 84 position vector components for the transducer at the pulse emit time.

As in previous solutions, ship positions at the receive times of the returning pulses were interpolated from GPS-derived ship positions spaced at 20 sec. In addition, the ship attitude was considered constant over the 3- to 6-sec time intervals following pulse emit. This simplifying assumption is generally supported by the data.

After the data were processed, the distances between transponder pairs were recomputed using the estimated WGS 84 coordinates and then differenced with the distances obtained from the acoustics-only solution. Figure 20 presents these distance differences as well as repeats the results presented in Figure 19. Although the modeling (3DF data) incorporated into this last solution (III) was expected to have enhanced the previous solution (designated as GPS 143), the mean difference in the baseline lengths actually increased from 15.2 to 16.8 m.

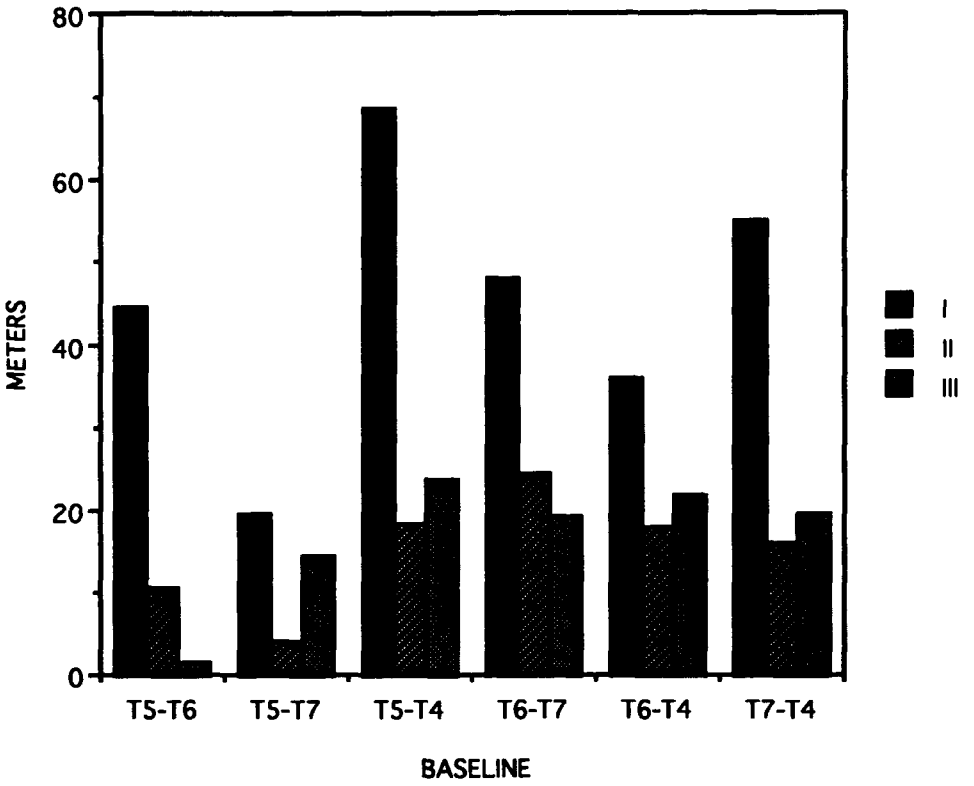

FIGURE 20. BASELINE LENGTH DIFFERENCES FOR SEVERAL PRELIMINARY SOLUTIONS

As a further step toward establishing a convergence between the acoustic data-only results and those supported by GPS, the procedure used to determine GPS ship coordinates at times of acoustic signal return was reexamined. Although several options for changing the approach existed, it was decided that the ship's speed and course-over-ground from the Ashtech 3DF receiver would be used. This approach would still minimize the number of files being processed, but would circumvent some of the weaknesses inherent with interpolating GPS 20-sec positions.

Since speed and course-over-ground were referenced to a local level frame, it was necessary to transform these quantities into the WGS 84 reference frame as was previously done for the 3DF attitude data. Then, assuming that these quantities were constant over the next 3 to 6 sec, the ship's displacement vector over each pulse emit/return interval was calculated. Transducer coordinates at receive times were then determined in WGS 84 and used in the acoustic data processing.

Figure 21 adds to the previous baseline comparisons the distance differences between this next solution (IV) incorporating 3DF attitude, speed, and course-over-ground and the acoustics-only solution. The mean baseline difference was now 6.9 m; however, the T6-T7 difference remained large.

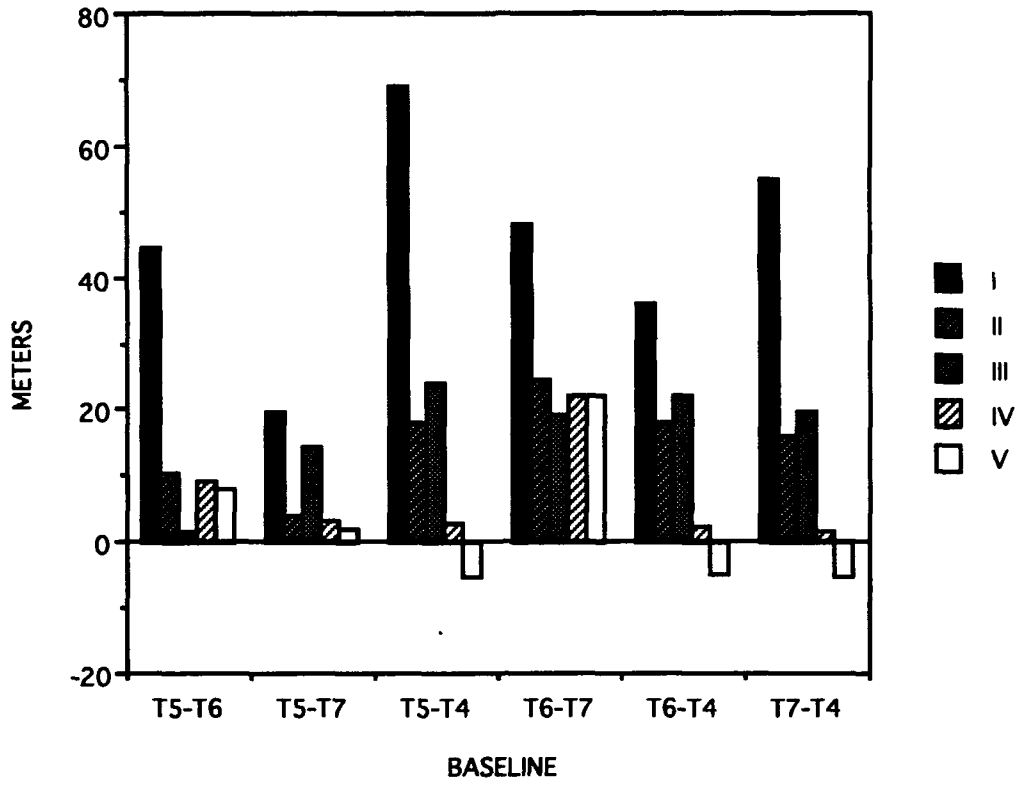

FIGURE 21. BASELINE LENGTH DIFFERENCES FROM ACOUSTICS-DATA-ONLY SOLUTION

Next, the observations from day 143, hour 0 were added to the data processing. These acoustics observations were supported by dual-frequency GPS positioning but were previously not processed because of difficulty in reading the file. The results of the baseline length comparisons from this solution (IV) with the acoustics-data-only solution are also given in Figure 21. The mean difference in baseline length was 2.9 m, with the T6-T7 baseline difference still excessive. The ship track pattern showing where this data (day 143, hour 0 to 3) was acquired is given in Figure 22, which can be contrasted with Figure 10.

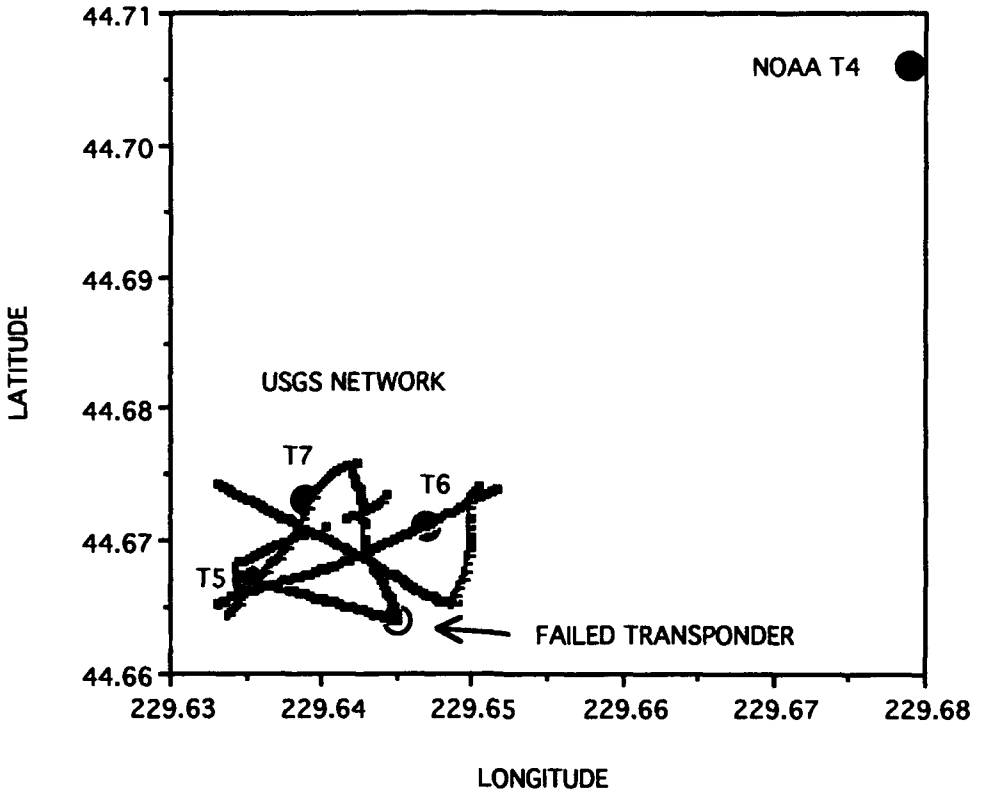

FIGURE 22. CALIBRATION TRACKS FOR DAY 143, HOUR 0–3

ACOUSTIC REFRACTION MODELING

As a final processing step, refraction corrections were estimated and applied to the acoustics data using a layered model for the sound velocity profile within the water column. This profile was developed from expendible bathythermograph observations collected in 1986 by NOAA in the vicinity of the USGS experiment. The profile is given in Table 6.

The acoustic pulse reaching each transponder arrives along a refracted path that depends on the temperature, pressure, and salinity within the water column. These variations are observed as a function of depth and are converted into a layered model parameterized by depth and sound velocity. Such layered profiles (see Figure 23) support ray tracing based on Shell's Law.[4]

TABLE 6. 1986 NOAA SOUND VELOCITY PROFILE IN WATER COLUMN NEAR JUAN DE FUCA RIDGE EXPERIMENT AREA

Depth (ft)	Velocity (ft/sec)
0.0	4954.40
3.281	4954.40
32.808	4953.41
65.617	4952.43
98.425	4950.46
131.234	4936.35
164.042	4915.68
246.063	4888.78
328.084	4882.87
492.126	4863.19
656.168	4863.85
984.252	4853.67
1312.336	4846.13
1640.420	4843.83
2460.630	4848.75
3280.840	4855.31
4101.050	4862.86
4921.260	4871.06
5741.470	4879.59
6561.680	4890.09
7381.890	4903.54

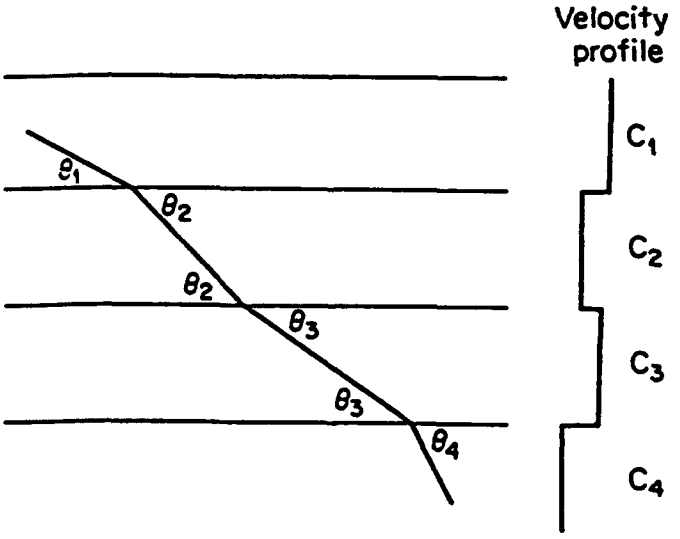

FIGURE 23. REFRACTION IN A LAYERED MEDIUM

As previously discussed, measurements within the water column were acquired during the deployment of the USGS transponders by instrumentation mounted onboard the deep-submersible *Turtle*. However, difficulty with software prevented the actual sound velocity profile from being available in time to support this data analysis. The NOAA profile given in Table 6 was used in the interim.

Each acoustic observation was corrected for refraction using the following procedure: signal emit and receive times were used to determine positions for the transducer in the WGS 84 reference frame based on GPS. Having approximate coordinates for the transponders in the same frame, as determined through previous processing, ray tracing through the profile in Table 6 was used to determine the amount of time the acoustic pulse took to reach then return from each transponder. Using approximate geometry, the angle of depression at the transducer to each transponder was determined to initiate the ray trace. The tracing terminated at the bottom depth of each transponder at an offset position from each instrument. These horizontal offsets were used to refine the depression angles at the surface; then ray tracing was repeated. This process was iterated until the traced rays reached each transponder location to within a meter. The process usually converged within three iterations for transponders T5, T6, and T7. For the more distant instrument T4, the process required additional care in adjusting the depression angle at each iteration and took around 10 iterations to converge.

Once the ray paths to and from the transponder were determined, the time of transit along the bent paths was calculated and differenced with an estimated time of transit along the straight-line geometric paths that would have been followed had the sound velocity profile been constant. The constant velocity used in this calculation was a weighted average determined for each transponder using the NOAA profile. The weights were based on the thickness of each profile layer with the bottom depth of each instrument terminating the profile in each calculation. The difference between the round-trip travel time along the bent rays and along the straight-line paths was used as an estimate of the refraction delay for each data point and was applied as a correction.

This approach for correcting for the effects of water column refraction was certainly not optimal since it incorporated certain assumptions and a NOAA profile that was only approximate. An alternate procedure for modeling the observation equation might circumvent some weaknesses in the assumptions. This alternate approach is summarized in the appendix.

Although not optimal, these refraction corrections were applied to the acoustics data available during day 143 when dual-frequency GPS observations supported ship positioning. Figures 24 and 25 provide one example of the effect that this refraction correction scheme had on the pre-adjustment data residuals. Figure 24 is a graph of residuals for transponder T5 on day 143, hour 1, prior to correction for refraction. Figure 25 provides the data residuals after refraction correction. It is evident that the refraction correction scheme has removed much of the high frequency noise on the acoustic data due to refraction effects. However, systematic effects are still present in the data. For instance, the step in the residuals occurring near data point 55 can be associated with a change in the GPS satellites being tracked. This *step* was also present in the residuals from hour 1 for the other transponders. It is suspected that much of the remaining systematic trends in the residuals are due to GPS positioning errors and inadequacies in the refraction model.

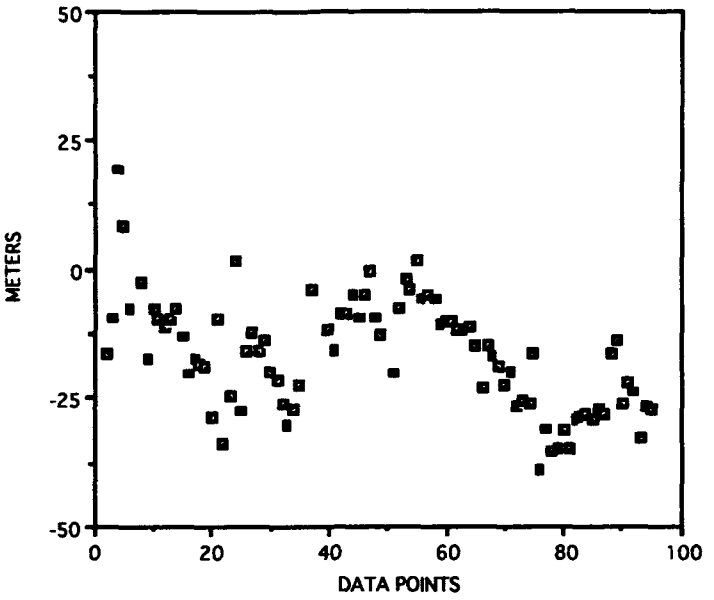

FIGURE 24. TRANSPONDER T5 PRE-ADJUSTMENT RESIDUALS WITH NO REFRACTION CORRECTION (DAY 143, HOUR 1)

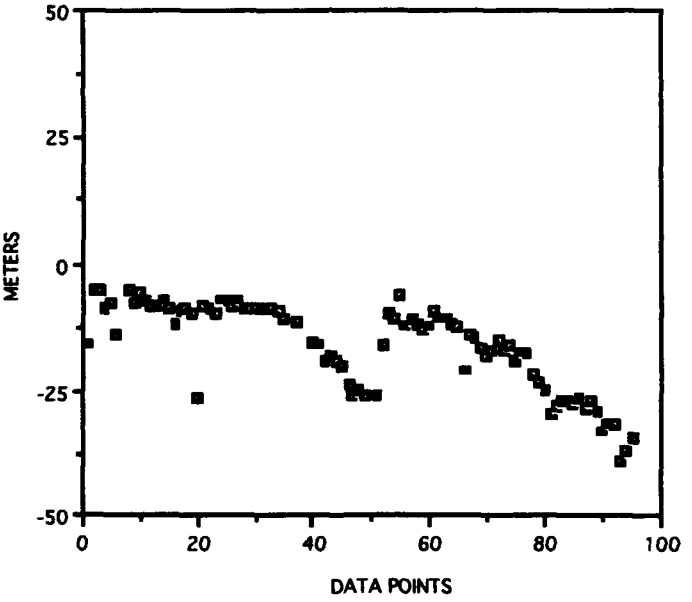

FIGURE 25. TRANSPONDER T5 PRE-ADJUSTMENT RESIDUALS WITH REFRACTION CORRECTION (DAY 143, HOUR 1)

After incorporating refraction correction into the adjustment model, data for day 143 was processed to determine the coordinates of the transponder network in the WGS 84 reference frame. All data having pre-adjustment residuals greater than 50 m were edited from the solution. An initial solution using this data included coordinate corrections for all four transponders. After data processing, residuals of fit and all combinations of baseline lengths were computed. Figure 26

illustrates the residuals after this adjustment for hour 1. Two points need to be made regarding Figure 26. First, systematic trends in the residuals remain, and second, numerous data residuals for the NOAA transponder T4 are aggregated (see box in figure) away from those for transponders T5, T6, and T7.

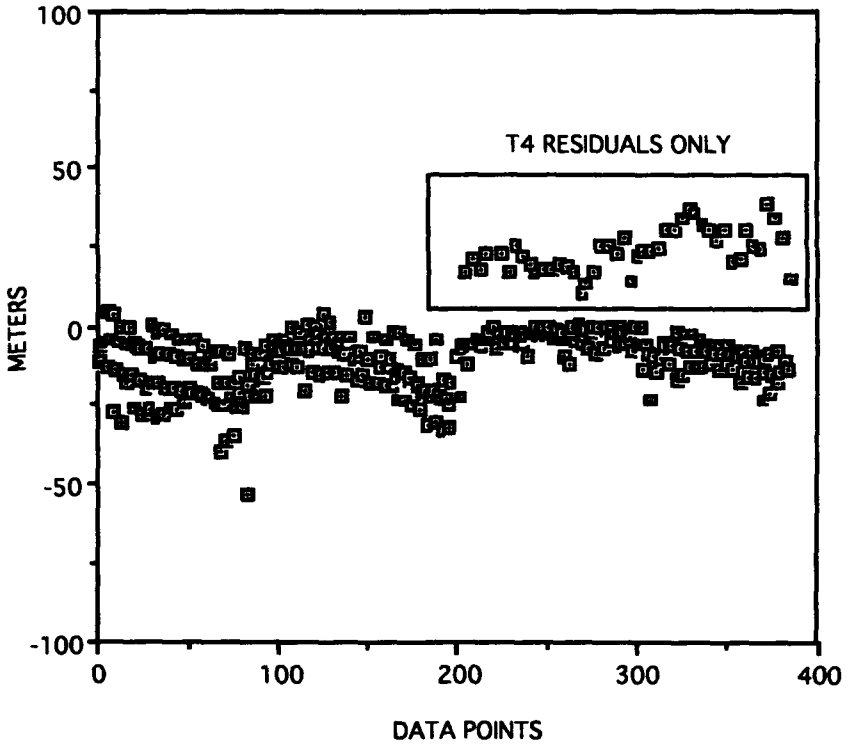

FIGURE 26. POST-ADJUSTMENT RESIDUALS FOR ALL TRANSPONDERS (DAY 143, HOUR 1)

Considering the data acquisition geometry presented in Figure 22 and the residuals associated with transponder T4, a second solution was made deleting all T4 data from the processing. It was known that the geometry (figure of merit) for the solution for the coordinates for T4 was much weaker and, because of the path lengths, the refraction corrections may be somewhat (more) suspect.

These last two solutions were designated *VIA* and *VIB*, respectively. Figure 27 depicts the resulting baseline length differences between several of the solutions discussed to this point using data supported by dual-frequency GPS tracking, GPS attitude, speed, and course-over-ground (see Table 5 for solution definition summary).

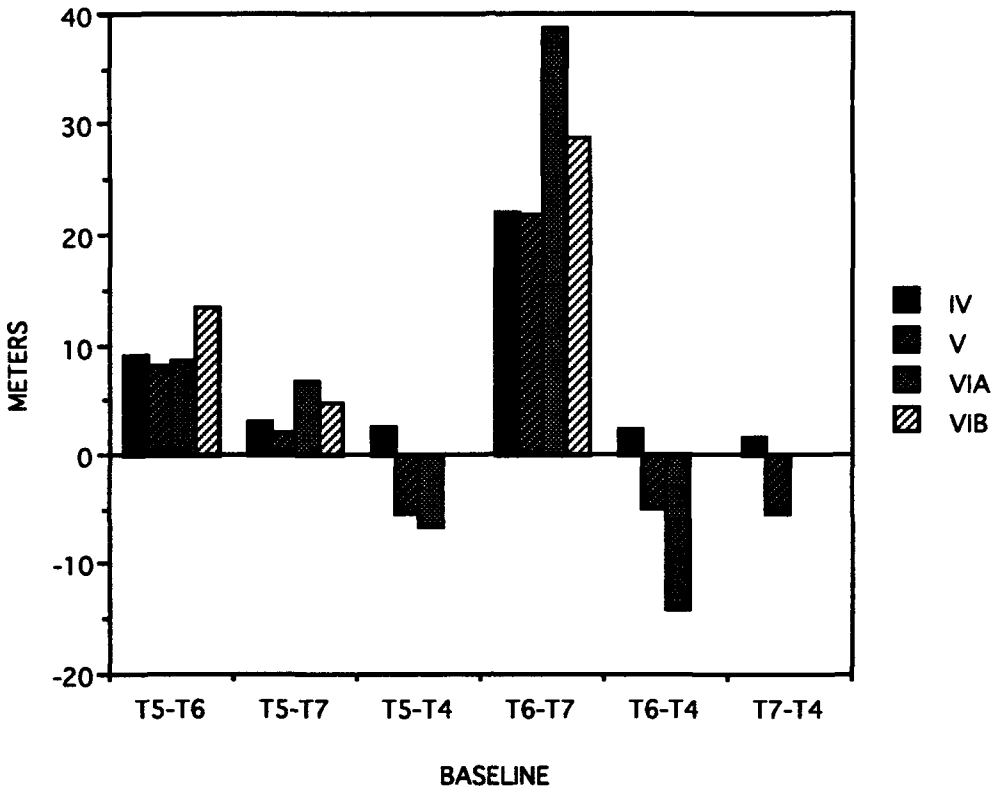

FIGURE 27. BASELINE DIFFERENCES BETWEEN VARIOUS GPS-SUPPORTED SOLUTIONS AND ACOUSTICS-ONLY SOLUTION

A comparison of the baseline solutions from V with VIA shows that the inclusion of refraction correction has an impact on the resulting lengths ranging from less than 1 m ((T5-T6) and (T7-T4)) to over 15 m (T6-T7). When a second solution with refraction correction was performed with T4 data removed, the change in the baselines between T5, T6, and T7 ranged from 2 to 10 m.

FINAL RESULTS AND CONCLUSIONS

To date, a number of solutions have been attempted, which incorporated differences in modeling and variations in the data sets. The solutions that combined GPS observables and acoustic measurements have been compared to an acoustics-data-only solution that determined ship and transponder positions in a local reference frame. Comparisons of different solutions were made using distances between transponders computed from estimated coordinates. Since these quantities are invariant with respect to coordinate system, they offer one method of determining consistency between solutions. Figure 28 provides the differences in the distances between transponders based on comparing the acoustics-data-only solution with seven other solutions derived using GPS and acoustics data. These latter solutions are in WGS 84 and were defined in Table 5. The six baseline combinations shown in Figure 28 were computed for all GPS-based

solutions with the exception of VIB, which did not include data from transponder T4. All data reductions using GPS were based on a constant sound velocity in the water column. For solutions VIA and VIB that constant was computed for each transponder using a 1986 NOAA sound velocity profile.

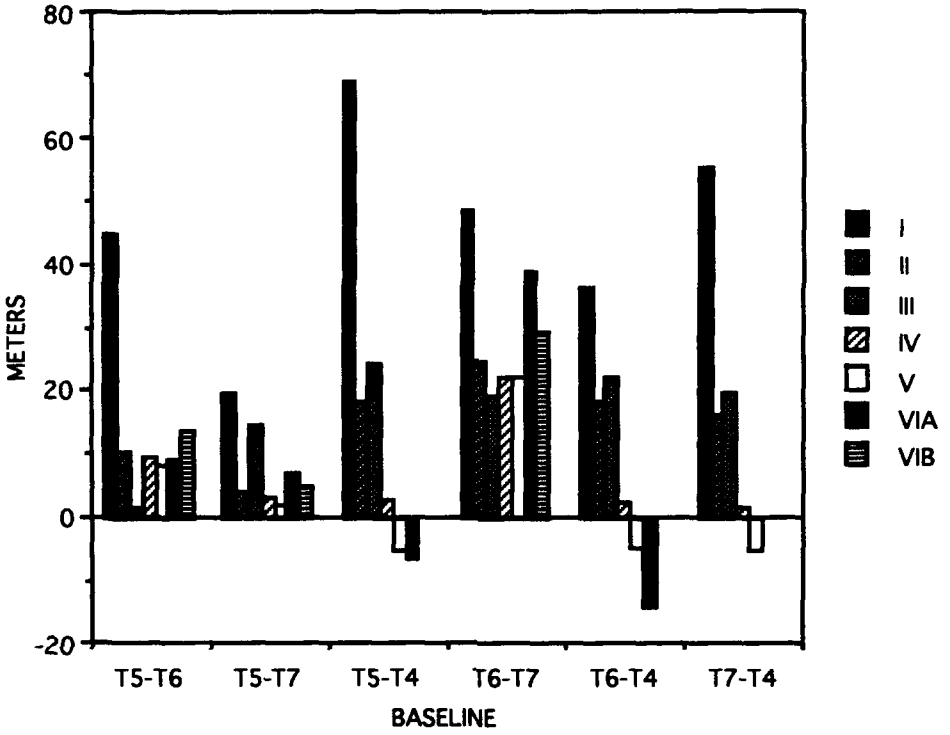

FIGURE 28. DIFFERENCES IN BASELINE LENGTHS WHEN VARIOUS GPS SOLUTIONS ARE COMPARED TO ACOUSTICS-ONLY SOLUTION

Solution V incorporated the full use of GPS data and, on average, agreed to 2.9 m with baseline lengths from the acoustics-data-only solution. However, due to the non-availability of dual frequency GPS data on day 142, the number of observations in solution V was significantly less than for the acoustics solution, which might account for the larger difference in the T6-T7 baseline length.

With the addition of refraction correction, it was shown that the baseline scale increased for the USGS network but decreased for baselines extending to T4. As this seemed suspect, a final solution VIB for T5, T6, and T7 coordinates was computed and is given in Table 7. The accuracy of this solution remains to be verified using directly measured acoustic distances that should be retrieved by the USGS on a subsequent site visit.

TABLE 7. USGS TRANSPONDER COORDINATES IN WGS 84 FROM SOLUTION VIB
(units in meters)

Unit	X	Y	Z
T5	-2941651.8	-3460767.0	4459469.7
T6	-2940709.0	-3461114.1	4459811.7
T7	-2941146.4	-3460589.4	4459938.1

RECOMMENDATIONS

The full potential for developing highly accurate geodetic coordinates from the USGS experiment was not realized for several reasons. Some of these were related to the data acquisition phase of the experiment, while others were a result of limitations imposed during data processing.

With respect to data acquisition, the following limitations were present in the data set.

- Simultaneous collection of acoustic and GPS support data did not always occur, resulting in the non-processing of significant amounts of acoustics data.
- GPS dual-frequency data on day 142 was lost.
- High-frequency acoustics measurements were commanded but not retrieved, preventing validation of geodetic positioning results.
- Data acquisition geometry (ship track pattern) during the calibration period did not yield a best figure of merit.
- An *in situ* water velocity profile was never provided to support data analysis.

Data analysis was limited by several of these factors and by the following:

- The processing technique to obtain GPS ship positions was not optimal and limited the accuracy of the results.
- Acoustics data were processed using an explicit representation for the observation equation that mapped transit time into distance using an assumed constant for the sound velocity.
- Acoustics data were corrected for refraction using a 1986 NOAA model.

Based on the circumstances surrounding data collection and processing limitations, it is recommended that the original data set be reprocessed at a later date using the actual water velocity profile and a more accurate GPS ship positioning scheme. In addition, it is recommended that during the next site visit that a similar data set be acquired in a manner that circumvents some of the previous data acquisition limitations.

REFERENCES

1. *Department of Defense World Geodetic System, 1984, Its Definition and Relationship with Local Geodetic Control*, DMA Technical Report 8350.2, 2d Ed.

2. Reilly, J.P.; Schwarz, C.R.; and Whiting, M.C., *The Ohio State University Geometric and Orbital (Adjustment) Program (OSUGOP) for Satellite Observations*, Report 190, Department of Geodetic Science and Surveying, The Ohio State University, Columbus, OH, 1972.

3. Leick, A., *GPS Satellite Surveying*, John Wiley & Sons, 1990.

4. Urick, R.J., *Principles of Underwater Sound,* 3d Ed., McGraw-Hill Book Company, 1983.

BIBLIOGRAPHY

Fell, P.J., *Seafloor Positioning: Survey Techniques, Mathematical Modeling and Estimation*, XX General Assembly of the International Union of Geodesy and Geophysics, Vienna, Austria, Aug 1991.

Fell, P.J., *A Survey of Marine Applications of the Global Positioning System*, 1992 Pacific Congress on Marine Technology (PACON), Kona, HI, 1-5 Jun 1992.

Fell, P.J., *Extending Geodetic Control onto the Seafloor*, Proceedings of the Marine Technology Society 1992 Symposium, Washington, D.C.

Fell, P.J. and Kumar, M., *Marine Applications of the Global Positioning System*, United Nations Conference for the Americas, New York, NY, Jan 1993 and 8th United Nations Regional Cartographic Conference for Africa, Kampala, Uganda, Feb 1993.

APPENDIX A

ESTIMATION APPROACH

ACOUSTIC OBSERVATION EQUATIONS

To first order the round-trip travel time T of the acoustic signal from the ship hull transducer to transponder T_i is modelled by the explicit equation

$$T_i = [R(S,T_i) + R(T_i,R_i)]/V_w + \Delta T_i + \Delta T_r \quad i = 1,2,3,4 \qquad \text{(A-1)}$$

where V_w is the average sound velocity in seawater; $R(S,T_i)$ is the geometric slant range from the transducer to transponder T_i at the emit time; $R(T_i,R_i)$ is the geometric slant range from the transponder to the transducer at the time of signal receipt; ΔT_i is the calibrated transponder electronic delay: and ΔT_r is a correction due to refraction in the water column.

ESTIMATION EQUATIONS

Acoustics data are processed sequentially, on a track-line basis. Transducer positions at pulse transmit and receive times are assumed to be known with an *a priori* uncertainty. The standard error on these ship positions σ_S or σ_{R_i} varies with the methods used to position the ship, geometry, and other factors.

For a given track of data, observations are grouped as discrete events. Each event consists of the data associated with a unique transmitted acoustic pulse and with the positions of up to four transponders and five ship locations. Each event is processed separately.

Given an event, the observation equation (A-1) is linearized about the *a priori* coordinates for the transponder array and about coordinates for the transducer positions (emit and receive):

$$V = AX + L \qquad \text{(A-2)}$$

Least squares normal equations are formed for the event, which include coordinate corrections for transponders T_i ($i = 1,2,3,4$) and ship positions S and R_i ($i = 1,2,3,4$). Separating transponder and ship position parameters, the normal equations are given in partitioned form as

$$(A^tWA)X + A^tWL = 0$$

or

$$NX + U = 0$$

where

$$A = [A_1, A_2]$$

$$L = L_o - L_b$$

$$X^t = [X_T, X_S\ X_R] = [X_1, X_2]$$

$$N = \begin{bmatrix} N_{11} & N_{12} \\ N_{21} & N_{22} \end{bmatrix}$$

$$U = \begin{bmatrix} U_1 \\ U_2 \end{bmatrix}$$

$$N_{11} = A_1{}^t W A_1 \qquad \text{(A-3)}$$

$$N_{12} = A_1{}^t W A_2$$

$$N_{21} = N_{12}{}^t$$

$$N_{22} = A_2{}^t W A_1$$

$$U_1 = A_1{}^t W L$$

$$U_2 = A_2{}^t W L$$

The design matrix *A* is developed by differentiating the observation equations with respect to all unknowns in each event:

$$\partial T_i/\partial X_{T_i} = [\partial R(S,T_i)/\partial X_{T_i} + \partial R(T_i,R_i)/\partial X_{T_i}]/v_w$$

$$= [(X_{T_i} - X_S)/R(S,T_i) + (X_{T_i} - X_{R_i})/R(T_i,R_i)]/v_w \quad X\text{-->}Y,Z \qquad \text{(A-4)}$$

$$\partial T_i/\partial X_S = [\partial R(S,T_i)/\partial X_S]/v_w = [(X_S - X_{T_i})/R(S,T_i)]/v_w \quad X\text{-->}Y,Z$$

$$\partial T_i/\partial X_{R_i} = [\partial R(T_i,R_i)/\partial X_{R_i}]/v_w = [(X_{R_i} - X_{T_i})/R(T_i,R_i)]/v_w \quad X\text{-->}Y,Z$$

The vector L contains the difference between observations computed with the model and the observed data.

After the normal equations are formed, *a priori* uncertainty on ship positions are used to constrain the solution. Weights are added to the normal equations, to the diagonals of N_{22}, computed from ship uncertainties.

The coordinate corrections for ship positions (S and R_i) are formally eliminated algebraically giving

$$(N_{11} - N_{12}(N_{22} + P_2)^{-1}N_{21})X_1 + (U_1 - N_{12}(N_{22} + P_2)^{-1}U_2) = 0 \qquad \text{(A-5)}$$

Each event j is processed in this fashion and the normal equations are accumulated for the track *k:*

$$N_k X_1 + U_k = 0$$

where

$$N_k = \sum_{j=1}^{n} (N_{11} - N_{12}(N_{22} + P_2)^{-1}N_{21})_j$$

$$U_k = \sum_{j=1}^{n} (U_1 - N_{12}(N_{22} + P_2)^{-1}U_2)_j \qquad \text{(A-6)}$$

A track solution for the coordinates of the transponders is given by:

$$X_1 = N_k^{-1}U_k \qquad \text{(A-7)}$$

Track normal equations are accumulated and a final solution is obtained after all data is processed as

$$X_1 = [P_x + \sum_{k=1}^{m} N_k]^{-1} [\sum_{k=1}^{m} U_k] \qquad \text{(A-8)}$$

where P_x is a weighting matrix developed from *a priori* uncertainty on the location of the array.

ALTERNATIVE OBSERVATION MODEL

The observation equation (A-1) presented earlier is an *explicit* formulation in terms of time and relies on a knowledge of the average sound speed in water to convert metric distances into transit times. The scale of the resulting network is directly influenced by the choice of this velocity v_W.

An alternative procedure is to treat the observation (transit time) as an *implicit* function of the coordinates for the transducer and transponders in the following way: Consider the time of transit T_i associated with an emitted pulse. The angle of depression α_{ST_i} at the emit time and the angles of depression $\alpha_{R_iT_i}$ at the receive times are functions of the positions of the transducer at points S and R_i and the positions of the transponders; i.e.,

$$\alpha_{ST_i} = \alpha(X_S, Y_S, Z_S, X_{T_i}, Y_{T_i}, Z_{T_i})$$

and $\qquad i=1,2,3,4 \qquad \text{(A-9)}$

$$\alpha_{R_iT_i} = \alpha(X_{R_i}, Y_{R_i}, Z_{R_i}, X_{T_i}, Y_{T_i}, Z_{T_i})$$

where $X_S, Y_S, Z_S, X_{R_i}, Y_{R_i}, Z_{R_i}, X_{T_i}, Y_{T_i}$, and Z_{T_i} are known approximately.

Using a water velocity profile as a function of depth, use ray tracing to determine the time of transit $T_r(S,T_i)$ and $T_r(R_i,T_i)$ using the angles α_{ST_i} and $\alpha_{R_iT_i}$ to initiate the process. Then the observed time T_i is related to T_r by

$$T_i = T_r(S,T_i) + T_r(R_i,T_i) + \Delta T_i \quad i = 1,2,3,4 \qquad \text{(A-10)}$$

The equation (A-10) for T_i represents the (implicit) observation equation.

In developing the estimation equations (A-3) using this approach, the partial derivatives (A-4) of T_i with respect to any of the coordinates $X_S, Y_S, Z_S, X_{R_i}, Y_{R_i}, Z_{R_i}, X_{T_i}, Y_{T_i}, Z_{T_i}$ are found by a variation of parameters procedure. That procedure is based on determining the changes in the computed observation T_i^c as a result of a sequence of small perturbations in the initial coordinate values. These are then used to develop the partial derivatives by the use of appropriate ratios.

DISTRIBUTION

	COPIES
DOD ACTIVITIES (CONUS)	
ATTN J SLATER (OPG)	1
W WOODEN (PRA)	1
T HENNIG (TI)	1
R SMITH (TIS)	2
DIRECTOR	
DEFENSE MAPPING AGENCY	
8613 LEE HIGHWAY	
FAIRFAX VA 22031-2137	
ATTN K BURKE (GG)	2
DIRECTOR	
DEFENSE MAPPING AGENCY	
AEROSPACE CENTER	
3200 S SECOND ST	
ST LOUIS MO 63118-3399	
ATTN R BARRETT (GDF)	1
B ROTH (GDF)	1
M KUMAR (GDF)	4
S MALYS (EG)	1
L KUNTZ (GDF)	1
DEFENSE MAPPING AGENCY	
SYSTEMS CENTER	
12100 SUNSET HILLS DR SUITE 200	
RESTON VA 22090-3221	
ATTN K COLLINS	1
J C LYNCH	1
SUPERINTENDENT	
DEPT OF OCEANOGRAPHY	
NAVAL POSTGRADUATE SCHOOL	
MONTEREY CA 93943	1
ATTN MAIL CODE 5110 (P VOGT)	1
NAVAL RESEARCH LABORATORY	
4555 OVERLOOK AVE SW	
WASHINGTON DC 20375-5320	
ATTN B ZIMMERMAN	1
J ACKERET	1
ASSOCIATE DIRECTOR SPACE PROGRAMS	
TEC	
FT BELVOIR VA 22060-5546	
ATTN CODE GG (S BARKER)	1
COMMANDING OFFICER	
NAVAL RESEARCH LABORATORY	
STENNIS SPACE CENTER	
BAY ST LOUIS MS 39522-5001	

	COPIES
DEFENSE TECHNICAL INFORMATION CTR	
CAMERON STATION	
ALEXANDRIA VA 22304-6145	12
NON-DOD ACTIVITIES (CONUS)	
ATTN G MADER	1
T SOLER	1
NGS NOS NOAA NCG143	
1315 EAST WEST HIGHWAY	
SILVER SPRING MD 20910	
ATTN MS 999 (C REISS)	5
UNITED STATES GEOLOGICAL SURVEY	
345 MIDDLEFIELD RD	
MENLO PARK CA 94025	1
ATTN P CEFOLA	1
DRAPER LABORATORY	
555 TECHNOLOGY SQUARE	
CAMBRIDGE SQUARE MA 02139	
ATTN J REILLY	1
DIRECTOR	
DEPT OF SURVEYING	
NEW MEXICO STATE UNIVERSITY	
BOX 30001 DEPT 3SUR	
LAS CRUCES NM 88003	
THE CNA CORPORATION	
PO BOX 16286	
ALEXANDRIA VA 22302-0268	1
ATTN I MUELLER	1
R RAPP	1
C JEKELI	1
B SCHAFFRIN	1
C GOAD	1
DEPARTMENT OF GEODETIC	
SCIENCE AND SURVEYING	
THE OHIO STATE UNIVERSITY	
1958 NEIL AVE	
COLUMBUS OH 43210-1247	

DISTRIBUTION (CONTINUED)

COPIES

NON-DOD ACTIVITIES (CONUS) (CONTINUED)

ATTN B VANGELDER 1
E MIKHAIL 1
S JOHNSON 1
DEPARTMENT OF
CIVIL ENGINEERING
PURDUE UNIVERSITY
WEST LAFAYETTE IN 47907-1284

ATTN T HERRING 54 618 1
MASSACHUSETTS INSTITUTE
OF TECHNOLOGY
CAMBRIDGE MA 02139

ATTN MS 238 625 (LICHTEN) 1
MS 238 540 (MELBOURNE) 1
JET PROPULSION LABORATORY
4800 OAK GROVE DRIVE
PASADENA CA 91109

ATTN CODE WRW402 (B SCHUTZ) 1
CENTER FOR SPACE RESEARCH
UNIVERSITY OF TEXAS AT AUSTIN
AUSTIN TX 78712

ATTN C KILGUS 2
APPLIED PHYSICS LABORATORY
JOHNS HOPKINS UNIVERSITY
JOHNS HOPKINS RD
LAUREL MD 20723-6099

ATTN R HILL 2
ARL UT
PO BOX 8029
10000 BURNET RD
AUSTIN TX 78713-8029

ATTN PROF ALFRED LEICK 1
DEPT OF SURVEYING ENGINEERING
UNIVERSITY OF MAINE
ORONO ME 04469

ATTN CODE 926 (O COLOMBO) 1
E PAVLIS 1
NASA
GODDARD SPACE FLIGHT CENTER
GREENBELT MD 20771

COPIES

ATTN LARRY HOTHEM 1
US GEOLOGICAL SURVEY
510 NATIONAL CENTER
RESTON VA 22092

ATTN GIFT AND EXCHANGE DIVISION 2
LIBRARY OF CONGRESS
WASHINGTON DC 20540

NON-DOD ACTIVITIES (EX-CONUS)

ATTN W SCHLUETER 1
SATELLITENBEOBACHTUNGSSTATION
WETTZELL
TECHNISCHE UNIVERSITAT MUNCHEN
D 8493 KOETZTING GERMANY

ATTN PROF GERARD LACHAPPELLE 1
DEPT OF SURVEYING ENGINEERING
THE UNIVERSITY OF CALGARY
2500 UNIVERSITY DR NW
CALGARY ALBERTA CANADA T2N 1N4

ATTN DR PER HELGE ANDERSEN 1
NORWEGIAN DEFENCE RESEARCH EST
PO BOX 25
N 2007 KJELLER NORWAY

ATTN PROF ERIK GRAFAREND 1
DEPT OF GEODETIC SCIENCE
UNIVERSITY OF STUTTGART
KEPLERSTRASSE 11
DW 7000 STUTTGART 1 GERMANY

ATTN DR J M DOW 1
ESA EUROPEAN SPACE OPERATIONS CENTRE
ROBERT BOSCH STRASSE 5
D 6100 DARMSTADT GERMANY

ATTN DR KAMIL EREN 1
UNPD
PO BOX 558
RIYADH 11421 SAUDI ARABIA

DISTRIBUTION (CONTINUED)

COPIES

NON-DOD ACTIVITIES (EX-CONUS) (CONTINUED)

ATTN G SEEBER 1
UNIVERSITY OF HANOVER
NEINBURGER STRASSE 5
D 30167 HANOVER GERMANY

ATTN N SAXENA 1
UNIVERSITY OF HAWAII AT MANOA
DEPT OF CIVIL ENGINEERING
HONOLULU HI 96822

ATTN J KOUBA 1
ENERGY MINES AND RESOURCES
GEODETIC SURVEY OF CANADA
OTTAWA CANADA K1A 0E9

ATTN C BOUCHER 1
INSTITUT GEOGRAPHIQUE NATIONAL
2 AVENUE PASTEUR
94160 SAINT MANDE FRANCE

ATTN G BEUTLER 1
W GUTNER 1
ASTRONOMICAL INSTITUTE OF BERNE
SIDLER STRASSE 5
CH 3012 BERNE SWITZERLAND

ATTN C REIGBER 1
DGFI ABT I
MARSTALLPLATZ 8
8000 MUNCHEN 22 FRG

INTERNAL

E231		3
E282	(SWANSBURG)	1
K10		1
K104	(FELL)	15
K12		5
K12	(SEAY)	15
K13		5
K14		5
K40		1
K43		2
N74	GIDEP	1
R		

REPORT DOCUMENTATION PAGE

Form Approved
OMB No. 0704-0188

1. AGENCY USE ONLY (Leave blank)	2. REPORT DATE	3. REPORT TYPE AND DATES COVERED
	April 1994	FINAL

4. TITLE AND SUBTITLE
Seafloor Positioning Across Juan de Fuca Ridge

5. FUNDING NUMBERS

6. AUTHOR(S)
Patrick Fell and C. Harris Seay

7. PERFORMING ORGANIZATION NAME(S) AND ADDRESS(ES)
Naval Surface Warfare Center, Dahlgren Division (Code K10)
17320 Dahlgren Rd
Dahlgren, VA 22448-5100

8. PERFORMING ORGANIZATION REPORT NUMBER
NSWCDD/TR-93/643

9. SPONSORING/MONITORING AGENCY NAME(S) AND ADDRESS(ES)

10. SPONSORING/MONITORING AGENCY REPORT NUMBER

11. SUPPLEMENTARY NOTES

12a. DISTRIBUTION/AVAILABILITY
Approved for public release; distribution is unlimited.

12b. DISTRIBUTION CODE

13. ABSTRACT *(Maximum 200 words)*

The results of an analysis of a complex data set acquired during the United States Geological Survey's Marine Crustal Deformation Study are presented. The experiment commenced in the spring of 1992 in a region of the Pacific known as the Juan de Fuca ridge. The experiment represents a first attempt to locally monitor plate dynamics in the marine environment over a period of years using a network of tripod-mounted, dual-frequency acoustic transponders. The aim is to collect time-series measurements of extension rates along the southern Juan de Fuca ridge. In addition, by collecting a combination of Global Positioning System satellite tracking data, low-frequency acoustics data, water column pressure, conductivity, and temperature at depth, it was possible to extend geodetic control from land onto the seafloor. The methods to accomplish this latter goal of the experiment are described, as well as the final results. Baseline comparisons between several of the solutions obtained during this analysis are presented along with recommendations for further analysis.

14. SUBJECT TERMS
Juan de Fuca ridge, geodetic positioning, seafloor, acoustics, Global Positioning System

15. NUMBER OF PAGES
52

16. PRICE CODE

17. SECURITY CLASSIFICATION OF REPORT	18. SECURITY CLASSIFICATION OF THIS PAGE	19. SECURITY CLASSIFICATION OF ABSTRACT	20. LIMITATION OF ABSTRACT
UNCLASSIFIED	UNCLASSIFIED	UNCLASSIFIED	SAR

GENERAL INSTRUCTIONS FOR COMPLETING SF 298

The Report Documentation Page (RDP) is used in announcing and cataloging reports. It is important that this information be consistent with the rest of the report, particularly the cover and its title page. Instructions for filling in each block of the form follow. It is important to ***stay within the lines*** to meet ***optical scanning requirements***.

Block 1. Agency Use Only *(Leave blank)*.

Block 2. Report Date. Full publication date including day, month, and year, if available (e.g. 1 Jan 88). Must cite at least the year.

Block 3. Type of Report and Dates Covered. State whether report is interim, final, etc. If applicable, enter inclusive report dates (e.g. 10 Jun 87 - 30 Jun 88).

Block 4. Title and Subtitle. A title is taken from the part of the report that provides the most meaningful and complete information. When a report is prepared in more than one volume, repeat the primary title, add volume number, and include subtitle for the specific volume. On classified documents enter the title classification in parentheses.

Block 5. Funding Numbers. To include contract and grant numbers; may include program element number(s), project number(s), task number(s), and work unit number(s). Use the following labels:

C	- Contract	**PR**	- Project
G	- Grant	**TA**	- Task
PE	- Program Element	**WU**	- Work Unit Accession No.

BLOCK 6. Author(s). Name(s) of person(s) responsible for writing the report, performing the research, or credited with the content of the report. If editor or compiler, this should follow the name(s).

Block 7. Performing Organization Name(s) and address(es). Self-explanatory.

Block 8. Performing Organization Report Number. Enter the unique alphanumeric report number(s) assigned by the organization performing the report.

Block 9. Sponsoring/Monitoring Agency Name(s) and Address(es). Self-explanatory.

Block 10. Sponsoring/Monitoring Agency Report Number. *(If Known)*

Block 11. Supplementary Notes. Enter information not included elsewhere such as: Prepared in cooperation with...; Trans. of...; To be published in... . When a report is revised, include a statement whether the new report supersedes or supplements the older report.

Block 12a. Distribution/Availability Statement. Denotes public availability or limitations. Cite any availability to the public. Enter additional limitations or special markings in all capitals (e.g. NOFORN, REL, ITAR).

DOD	- See DoDD 5230.24, "Distribution Statements on Technical Documents."
DOE	- See authorities.
NASA	- See Handbook NHB 2200.2
NTIS	- Leave blank

Block 12b. Distribution Code.

DOD	- Leave blank.
DOE	- Enter DOE distribution categories from the Standard Distribution for Unclassified Scientific and Technical Reports.
NASA	- Leave blank.
NTIS	- Leave blank.

Block 13. Abstract. Include a brief ***(Maximum 200 words)*** factual summary of the most significant information contained in the report.

Block 14. Subject Terms. Keywords or phrases identifying major subjects in the report.

Block 15. Number of Pages. Enter the total number of pages.

Block 16. Price Code. Enter appropriate price code ***(NTIS only)***

Block 17.-19. Security Classifications. Self-explanatory. Enter U.S. Security Classification in accordance with U.S. Security Regulations (i.e., UNCLASSIFIED). If form contains classified information, stamp classification on the top and bottom of this page.

Block 20. Limitation of Abstract. This block must be completed to assign a limitation to the abstract. Enter either UL (unlimited or SAR (same as report). An entry in this block is necessary if the abstract is to be limited. If blank, the abstract is assumed to be unlimited.